



**HAL**  
open science

# Monotonic axial compressive behaviour and confinement mechanism of square CFRP-steel tube confined concrete

Yanlei Wang, Gaochuang Cai, Amir Si Larbi, Daniele Waldmann,  
Konstantinos Daniel Tsavdaridis, Jianghua Ran

## ► To cite this version:

Yanlei Wang, Gaochuang Cai, Amir Si Larbi, Daniele Waldmann, Konstantinos Daniel Tsavdaridis, et al.. Monotonic axial compressive behaviour and confinement mechanism of square CFRP-steel tube confined concrete. *Engineering Structures*, 2020, 217, 10.1016/j.engstruct.2020.110802 . hal-04084607

**HAL Id: hal-04084607**

**<https://hal.science/hal-04084607v1>**

Submitted on 28 Jan 2025

**HAL** is a multi-disciplinary open access archive for the deposit and dissemination of scientific research documents, whether they are published or not. The documents may come from teaching and research institutions in France or abroad, or from public or private research centers.

L'archive ouverte pluridisciplinaire **HAL**, est destinée au dépôt et à la diffusion de documents scientifiques de niveau recherche, publiés ou non, émanant des établissements d'enseignement et de recherche français ou étrangers, des laboratoires publics ou privés.



UNIVERSITY OF LEEDS

This is a repository copy of *Monotonic axial compressive behaviour and confinement mechanism of square CFRP-steel tube confined concrete*.

White Rose Research Online URL for this paper:  
<https://eprints.whiterose.ac.uk/161167/>

Version: Accepted Version

---

**Article:**

Wang, Y, Cai, G, Si Larbi, A et al. (3 more authors) (2020) Monotonic axial compressive behaviour and confinement mechanism of square CFRP-steel tube confined concrete. *Engineering Structures*, 217. 110802. p. 110802. ISSN 0141-0296

<https://doi.org/10.1016/j.engstruct.2020.110802>

---

© 2020, Elsevier. This manuscript version is made available under the CC-BY-NC-ND 4.0 license <http://creativecommons.org/licenses/by-nc-nd/4.0/>.

**Reuse**

This article is distributed under the terms of the Creative Commons Attribution-NonCommercial-NoDerivs (CC BY-NC-ND) licence. This licence only allows you to download this work and share it with others as long as you credit the authors, but you can't change the article in any way or use it commercially. More information and the full terms of the licence here: <https://creativecommons.org/licenses/>

**Takedown**

If you consider content in White Rose Research Online to be in breach of UK law, please notify us by emailing [eprints@whiterose.ac.uk](mailto:eprints@whiterose.ac.uk) including the URL of the record and the reason for the withdrawal request.



[eprints@whiterose.ac.uk](mailto:eprints@whiterose.ac.uk)  
<https://eprints.whiterose.ac.uk/>

# 1 **Monotonic axial compressive behaviour and confinement** 2 **mechanism of square CFRP-steel tube confined concrete**

3  
4 **Yanlei Wang<sup>1</sup>, Gaochuang Cai<sup>2,3\*</sup>, Amir Si Larbi<sup>3</sup>, Danièle Waldmann<sup>4</sup>, Konstantinos Daniel**  
5 **Tsavidaridis<sup>5</sup>, Jianghua Ran<sup>1</sup>**

6  
7 1. State Key Laboratory of Coastal and Offshore Engineering, School of Civil Engineering, Dalian  
8 University of Technology, Dalian 116024, P.R. China.

9 2. Dept. of Architecture, Faculty of Eng., Fukuoka University, Fukuoka, 814-0180, Japan.

10 3. Univ Lyon, Ecole Nationale d'Ingénieurs de Saint-Etienne (ENISE), Laboratoire de Tribologie et de  
11 Dynamique des Systèmes (LTDS), UMR 5513, 58 Rue Jean Parot, 42023 Saint-Etienne Cedex 2,  
12 France.

13 4. Laboratory of Solid Structures, University of Luxembourg, Luxembourg, Luxembourg.

14 5. School of Civil Engineering, University of Leeds, Leeds LS2 9JT, UK

15  
16 \*Corresponding author: Gaochuang Cai

17 Email: gaochuang.cai@enise.fr

## 18 19 **Abstract**

20 Steel tube confined concrete (STCC) is widely used in the vertical members of high-rise buildings  
21 such as columns. The axial load is not directly resisted by the steel tube in STCC, but is resisted via  
22 the interfacial frictional stress between steel tube and concrete core, which is different with that of  
23 concrete filled steel tube (CFT) members and would effectively suppress the outward local buckling of  
24 steel tube at early stage. Recently, fibre-reinforced polymer (FRP) confined STCC presents a potential  
25 to enhance the ductility and durability of such vertical elements. This paper presents an experimental  
26 study on monotonic axial compressive behaviour of carbon FRP (CFRP) confined STCC (CFRP-  
27 STCC) stub column and an analytical study on the confinement mechanism of and the ultimate axial  
28 bearing capacity of the elements. A three-stage confinement mechanism involving the different  
29 contributions of the steel tube and the CFRP wrap in CFRP-STCC elements was proposed based on  
30 the test results. A prediction model of the ultimate axial bearing capacity of CFRP-STCC stub  
31 columns was developed subsequently. Results show that the presence of CFRP wrap enhances  
32 effectively the load-bearing capacity and the ductility of steel tube confined plain concrete and  
33 reinforced concrete elements, and significantly prevents the local buckling of the steel tubes in the

34 elements. The proposed prediction model of ultimate axial bearing capacity assesses test results with a  
35 great agreement.

36 **Keywords:** FRP confined concrete; Steel tube confined concrete; Constitutive model; Confinement  
37 mechanism; axial compressive behaviour

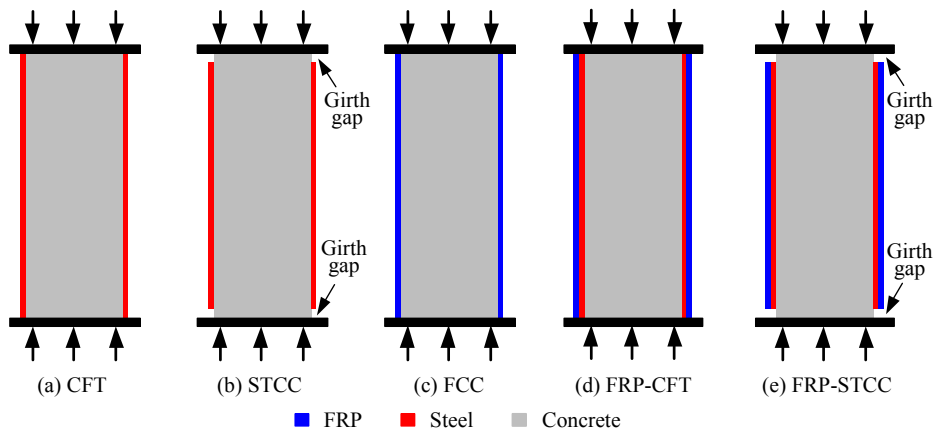
38

### 39 **1. Introduction**

40 Reinforced concrete (RC) structures still are widely used in most of the earthquake-prone zones of the  
41 world. Numerous studies have revealed that a sufficient confinement can significantly enhance the  
42 ductility of RC elements subjected to seismic loads. To achieve an effective confinement, various  
43 methods and technical provisions have been developed according to a series of experimental  
44 laboratorial studies and earthquake field surveys. Among them, an effective and easily implemented  
45 method at the early stage of the previous research is using steel stirrups or hoops with a smaller  
46 spacing at the hinge zones of RC elements such as RC columns.

47 In order to further improve the bearing capacity and seismic performance of RC columns, concrete-  
48 filled steel tube (CFT) column (Fig.1a) has been developed and widely applied in civil engineering  
49 due to the effective confinement of steel tube in such elements [1]. However, the steel tube of CFT  
50 must be thick to avoid its potential local buckling [2]. Steel tube confined concrete (STCC) column  
51 (Fig. 1b) is an innovative type of composite columns [3-9], in which the main difference with CFT  
52 column is that the steel tube is disconnected to both ends of the column (Fig. 1b). There are two main  
53 benefits obtained from this difference of STCC columns. One is the construction simplification of  
54 beam-column joints because that steel tube does not need to pass through the joint zone, which has  
55 been illustrated by the literature [9]. Another is that the potential local buckling of steel tube can be  
56 effectively avoided or delayed as STCC elements are under compressive load. This is because that the  
57 steel tube in STCC does not resist directly axial load and mainly provides a confinement to concrete  
58 core. It means the thickness of steel tube in STCC can be controlled compared with that of CFT in  
59 order to archive the same load-bearing capacity. **The STCC elements have the potential of wide**  
60 **applications in new construction.** It should be noted that, however, the steel tube in STCC still resists  
61 certain axial load from compressive load via the interfacial friction between steel tube and concrete  
62 core. But the interfacial friction can be reduced by smoothing the inner surface of steel tube (i.e. oil  
63 treatment). However, the main concerns of CFT and STCC elements are the durability issues of  
64 external steel tube (i.e. its resistance to corrosion) when they are subjected to aggressive environments.  
65 **The conventional corrosion protection for steel tube is additional coating. However, some small**

66 defects could occur in the coating process or the use of steel tubes [2] such as cyclic loads or fatigue  
 67 loads, which then can cause the pitting corrosion of the tube and then result in the subsequently large  
 68 area corrosion of the steel tube. Therefore, it is desirable to explore alternative corrosion protection for  
 69 steel tube.



70

**Fig. 1.** Schematic diagram of different confined concrete columns.

71

72

73 Fibre reinforced polymer (FRP) has been widely applied in civil engineering due to its high strength,  
 74 light weight, good fatigue resistance, and especially excellent durability [10-17]. FRP confined  
 75 concrete (FCC) column (Fig. 1c) is one of important applications of FRP material in civil engineering  
 76 to improve the bearing capacity and ductility of concrete core [18-19]. FRP material provides a new  
 77 choice for steel tube to resist corrosion by wrapping FRP layer on the outside of steel tube. To  
 78 improve the durability of the outer steel tube of CFT and STCC elements under aggressive  
 79 environments, and to avoid or delay the early age local buckling of steel tube of CFT elements, several  
 80 researchers proposed using FRP wrap to confine CFT (FRP-CFT, Fig. 1d) [20-28] or STCC (FRP-  
 81 STCC, Fig. 1e) [29] elements. FRP-CFT and FRP-STCC elements are two innovative composite  
 82 elements, which benefit the advantages of both CFT and STCC. The outer FRP wrap/confining can  
 83 effectively prevent the potential corrosion problem of outer steel tube under aggressive environments  
 84 and enhance the bearing capacity of CFT/STCC. This means that the same bearing capacity still can  
 85 be reached in the composite elements when the thickness of steel tube is reduced, which can reduce  
 86 the manufacturing difficulty of thick steel tube. Meanwhile, it also can delay or even avoid the  
 87 cracking of the welding seam of the steel tube because of the effective confinement of the outer FRP  
 88 wrap. It should be admitted that the brittle fracture of FRP material at its ultimate state may lead to a  
 89 sudden failure of FRP-STCC elements, however, the FRP wrap can provide the STCC higher  
 90 confinement which could significantly improve the bearing capacity and the peak strain of the STCC

91 **elements.** Due to the large difference of thermal expansivity between FRP and steel, large temperature  
92 difference is considered as a challenge for the interface adhesive in FRP-CFT and FRP-STCC  
93 elements. This environment may cause the degradation of structural performance of the elements, thus  
94 endangers the service life span of the structures. Therefore, **high toughness** adhesives are suggested to  
95 fabricate the FRP wrap in FRP-CFT and FRP-STCC elements to delay the deterioration of their  
96 structural behaviours caused by a large temperature difference. **Moreover, the balance between the**  
97 **toughness of the adhesives and their glass transition temperatures should be considered, to avoid the**  
98 **serviceability problems of the elements at higher service temperatures due to low glass transition**  
99 **temperature.** On the other hand, the aging problem of external FRP wrap due to sunlight (mainly  
100 Ultraviolet light) [30], temperature, and humidity is the main concern of the durability of FRP-  
101 confined or -strengthened structures. To fix this issue, a surface treatment such as coating of FRP wrap  
102 is suggested in practical application. **As new corrosion protection of steel, the cost of FRP wrap in**  
103 **FRP-STCC elements is more expensive than those of the conventional corrosion protections of steel,**  
104 **due to the high price of FRP materials and additional coating materials to resist the aging problems of**  
105 **FRP. However, FRP wrap is also expected to improve the structural performance (the bearing capacity,**  
106 **peak strain and local buckling, etc.) of STCC elements with the benefits of the material advantages.**

107 Compared to STCC and FCC elements, limited studies were conducted [2,29,31] to understand the  
108 structural behaviour of FRP-STCC elements such as the effectiveness of FRP wrap to prevent the  
109 failure provoked by local damage of steel tube. Lin [29] studied the structural behaviour of circular  
110 glass FRP (GFRP) confined STCC (GFRP-STCC) columns to investigate the effects of the type of and  
111 the number of layers of FRP wrap, stirrup ratio, and loading type. It was reported that FRP wrap, steel  
112 tube, and reinforcements in STCC elements all can enhance significantly the axial load-carrying  
113 capacity and the ductility of the elements [28]. Huang [31] experimentally investigated the cyclic  
114 constitutive behaviour of circular GFRP-STCC columns and proposed a design model to predict the  
115 compressive behaviour of the confined concrete. Xu *et al* [2] tested circular carbon FRP (CFRP)  
116 confined STCC (CFRP-STCC) stub columns to investigate their eccentric compressive behaviour and  
117 presented *N-M* interaction relationship by a plastic stress distribution method. However, up to now,  
118 only a few parameters were studied to understand their effects of FRP wrap on the constitutive  
119 behaviour of confined concrete [28,31] and no research was reported about square FRP-STCCs.  
120 However, both constitutive behaviour and confinement mechanism are considered very important to  
121 the structural analysis of FRP-STCC structures. To develop a more reliable analysis constitutive model,  
122 more test studies on square FRP-STCC elements are needed to establish the stress-strain law of square  
123 FRP-STCCs.

124 The main objectives of the paper are to study the monotonic axial compressive behaviour of square  
125 CFRP-STCCs and to analyse the confinement mechanism of square steel tube and CFRP wrap in the  
126 confined concrete stub columns. Although CFRP materials are more expensive and have a small  
127 fracture strain and may cause potential galvanic corrosion issues, however, as a start of the study on  
128 the confined STCC elements, CFRP was first selected among commonly used FRP materials (i.e.  
129 CFRP, GFRP, aramid FRP, and basalt FRP). The main reasons are: (1) The elastic modulus of CFRP  
130 materials is close to that of steel materials, which meaning it is easier to work together with the steel  
131 tube, compared with the other FRP materials. (2) CFRP materials have a higher strength-weight ratio,  
132 which means it has a high potential to effectively improve the confinement of the inside concrete in  
133 STCC elements. (3) The basic research conclusions of CFRP-STCC are also applicable to those of the  
134 STCC confined by other FRP materials due to the inherent linear elastic response of FRP materials.  
135 Based on the experimental study, a calculation model was proposed to assess the axial bearing  
136 capacity of CFRP-STCC stub columns. The investigation mainly includes failure modes, load-  
137 deformation behaviour, the influence of main parameters (the number of layers of CFRP wrap, width-  
138 to-thickness ratio of steel tube, corner radius at sectional corner), and confining stress analysis of  
139 CFRP-STCCs.

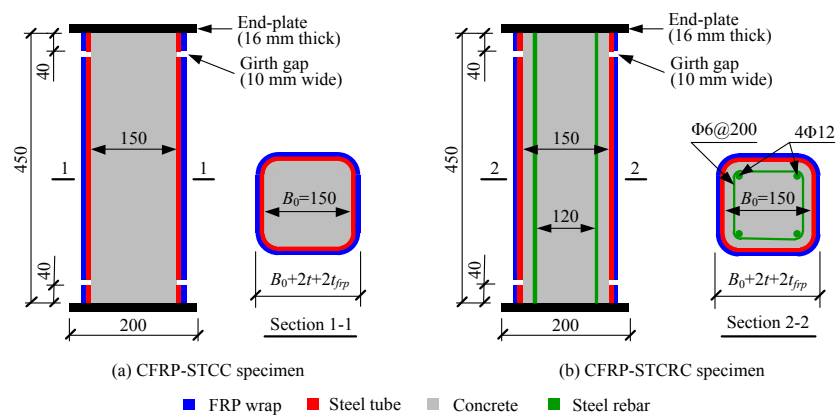
140

## 141 **2 Test investigation**

### 142 2.1 Test specimens

143 In this study, total 23 specimens were prepared and tested, including 11 square CFRP-steel tube  
144 confined plain concrete (CFRP-STCC) stub columns, 3 square steel tube confined plain concrete  
145 (STCC) stub columns, 6 square CFRP-steel tube confined reinforced concrete (CFRP-STCRC) stub  
146 columns and 3 square steel tube confined reinforced concrete (STCRC) stub columns. The height-to-  
147 width ratio ( $H/B_0$ ) of all specimens is 3.0. Fig. 2 gives the details of the test specimens. The volumetric  
148 ratios of the longitudinal reinforcement ( $4\Phi12$ ) and steel stirrup ( $\Phi6@200$ ) of confined RC specimens  
149 were 2.0% and 0.4%, respectively. The steel stirrups in the related specimens were only used to fix the  
150 longitudinal reinforcements, and the hoop confinement of them to the concrete core was ignored in the  
151 later analysis. In order to ensure that applied axial load was transferred uniformly to the internal  
152 longitudinal reinforcement in the specimens, both ends of each longitudinal rebar were welded to the  
153 bottom and top steel plates of each specimen (see Fig. 2b), respectively. In order to guarantee that the  
154 steel tube does not directly bear axial load in each specimen, a ring with a length of 10 mm was cut  
155 after casting from both ends of steel tube (40 mm from the ends), forming two girth gaps in each  
156 specimen shown in Fig.2. A wet lay-up process was used to conduct CFRP wrap to steel tubes in the

157 specimens. Before CFRP was wrapped, the floating rust and impurities on the surface of the steel  
 158 tubes were removed with a fine sandpaper and using an alcohol treatment. CFRP sheets with the same  
 159 height as that of the steel tube were then uniformly and tightly wrapped on the outer surface of the  
 160 steel tube with an epoxy adhesive. The overlapping length of CFRP sheets was 120 mm according to  
 161 the Chinese Code (GB 50608-2010) [32], which was arranged to cover one of the welding seams of  
 162 steel tube (seen Fig. 3). The details of each specimen are listed in Table.1. The studied corner radiiuses  
 163 of the steel tubes were 10 mm, 20 mm, 30 mm, as PC-D-2-2(10), PC-B-2-2 and PC-D-2-2(30)  
 164 specimens listed in the table, respectively.



165  
 166 **Fig. 2.** Details of test specimens (Units in mm).

167  
 168 **Table.1** Details of test specimens

Types	Specimen no.	Steel tube		CFRP		$R$ /mm	Cross section
		$t$ /mm	$B/t$	$n$	$t_{frp}$ /mm		
	PC-A-1-0	1	152	0	0	20	
	PC-A-1-1	1	152	1	0.167	20	
	PC-A-1-2	1	152	2	0.334	20	
	PC-A-1-3	1	152	3	0.501	20	
	PC-B-2-0	2	77	0	0	20	
Confined plain concrete (PC)	PC-B-2-1	2	77	1	0.167	20	
	PC-B-2-2	2	77	2	0.334	20	
	PC-B-2-3	2	77	3	0.501	20	
	PC-C-3-0	3	52	0	0	20	
	PC-C-3-1	3	52	1	0.167	20	
	PC-C-3-2	3	52	2	0.334	20	
	PC-C-3-3	3	52	3	0.501	20	
	PC-D-2-2(10)	2	77	2	0.334	10	
	PC-D-2-2(30)	2	77	2	0.334	30	



	RC-A-1-0	1	152	0	0	20	
	RC-A-1-2	1	152	2	0.334	20	
	RC-A-1-3	1	152	3	0.501	20	
Confined RC	RC-B-2-0	2	77	0	0	20	
	RC-B-2-2	2	77	2	0.334	20	
	RC-B-2-3	2	77	3	0.501	20	
	RC-C-3-0	3	52	0	0	20	
	RC-C-3-2	3	52	2	0.334	20	
	RC-C-3-3	3	52	3	0.501	20	

169 Note:  $B/t$  is the width-to-thickness ratio of steel tube;  $t$  and  $t_{frp}$  are the thickness of steel tube and CFRP  
170 wrap, respectively;  $n$  is the number of layers of CFRP;  $R$  is the corner radius of steel tube.

171

## 172 2.2 Material properties

173 The elastic modulus, the yield load, and the ultimate tensile strength of the used steel tubes were  
174 measured according to the Chinese Code, GB/T 228-2002 [33]. The test results are shown in Table 2.

175 The longitudinal rebars were HRB 335 rebars with a diameter of 12 mm, a measured yield strength of  
176 378 MPa and an ultimate tensile strength of 540 MPa. A standard commercial concrete with a  
177 maximum coarse aggregate size of 10.0 mm was used in all specimens which was supplied by a local  
178 company. Three cylinders of  $\varnothing 150 \times 300$  mm were tested under axial compression to define the  
179 compressive strength of used concrete. The average compressive strength of unconfined concrete was

180 55.4 MPa. The related material properties of CFRP sheet (surface density: 300 g/m<sup>2</sup>, provided by  
181 Toray Co., Ltd, Japan), and of epoxy adhesive (provided by Dalian Kaihua New Technology  
182 Engineering Co., Ltd, China), were provided by manufacturers and listed in Table 2. In order to avoid  
183 potential galvanic corrosion between CFRP wrap and steel tube in practical application, a thin  
184 insulating layer (i.e. Glass FRP) must be wrapped firstly before wrapping CFRP sheet on steel tube.

185 However, the insulating layer was not applied in the study considering the test is short-term without  
186 such galvanic corrosion issue. **Although the CFRP-STCC elements proposed in this paper are relative  
187 complex, consisting of steel rebars, concrete, steel tube, GFRP, CFRP, epoxy layers, and an additional  
188 protection layer, it is one of the ways to effectively solve the corrosion problem of steel tube. And if  
189 CFRP is replaced by GFRP in the elements, the additional insulating layer is not needed. Moreover, to  
190 resist the steel corrosion, similar technologies using FRP wrap on steel tube had already been applied  
191 in the structures with steel piles located in several harbours in China [31]. These projects preliminarily  
192 proved the effectiveness of the FRP wrap to resist steel corrosion of the structures. Therefore, as one  
193 of the treatments of durability and effective confinement methods, the proposed FRP-STCC elements  
194 present the potential of wide applications in practical projects to address the corrosion problem of steel**

195 tube and improve the structural performance of the elements. In addition, to simplify the analysis, the  
 196 axial compressive behaviour contributed from the thin GFRP insulating layer can be omitted due to  
 197 the layer can be very thin in the practical application of CFRP-STCC elements.

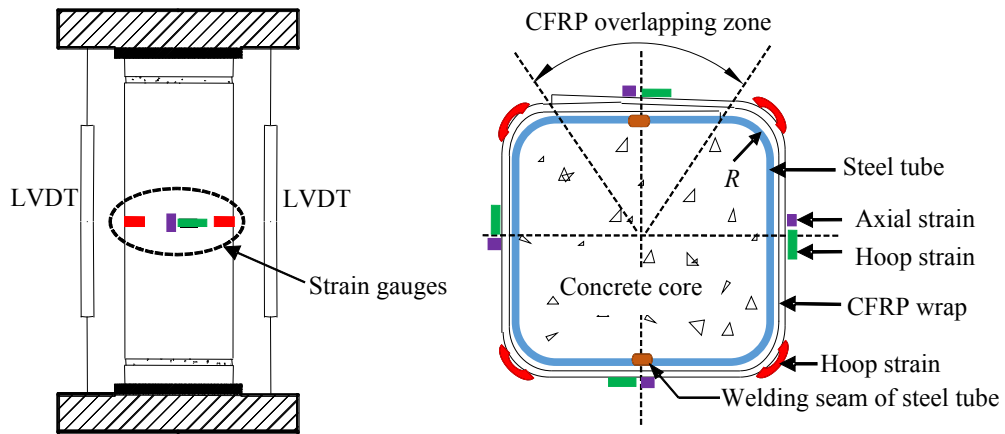
198 Table.2 Material properties of steel tube, CFRP sheet and epoxy adhesive

Materials	Nominal thickness /mm	Elastic modulus /GPa	Yield tensile strength /MPa	Ultimate tensile strength /MPa	Elongation /%
Steel #1	1.0	210	188	330	-
Steel #2	2.0	204	192	345	-
Steel #3	3.0	205	200	323	-
CFRP	0.167	245	-	4077	1.51
Epoxy	-	>2.5	-	>40	>1.80

199

### 200 2.3 Loading and measurement

201 The measurement and setup of the test are presented in Figs. 3 and 4. A monotonic axial compressive  
 202 loading was applied on each specimen by a 5000 kN hydraulic compressive machine (see Fig. 4),  
 203 which was controlled by vertical displacement with a rate of 0.5mm per minute referring to the  
 204 literature [1]. The axial compressive load was measured by a load cell placed on the top of the  
 205 specimens. Two linear variable displacement transducers (LVDTs) with a measurement range of  
 206 50 mm were arranged symmetrically on the diagonal direction of the test specimens to measure the  
 207 vertical displacement of stub columns, as shown in Figs. 3 and 4. Twelve strain gauges with a gauge  
 208 length of 20 mm were installed on CFRP wrap to measure the axial and hoop strains of CFRP wrap  
 209 and steel tube at the mid-height of the test specimens, as shown in Fig. 3. Since CFRP wraps were well  
 210 bonded to steel tubes with epoxy adhesive, the inner steel tube was considered to work together with  
 211 the outer CFRP wrap without interfacial slippage. Therefore, the strains of the inner steel tube were  
 212 assumed to be the same as those of the outer CFRP wrap. The strain and load information were  
 213 collected synchronously at an acquisition frequency of 1.0 Hz.



214  
215

**Fig. 3.** Layout of LVDTs and strain gauges in the specimens.



216  
217

**Fig. 4.** Test setup.

### 218 3 Test observations and analyses

#### 219 3.1 Failure modes

220 The damage and failure modes of the steel tube confined concrete specimens and the CFRP-steel  
 221 tube confined concrete specimens are shown in Fig. 5. In the steel tube confined concrete columns, the  
 222 concrete cover at the ends of steel tube experienced sporadic crushing or spalling when approaching  
 223 the peak loads of the columns. When the axial load dropped to around 70% of their peak load, the steel  
 224 tube near the middle section suffered a significant outward local buckling. After removing the steel  
 225 tubes, several obvious shear damages were observed in the steel tube confined plain concrete  
 226 specimens, as shown in Fig. 5 (a), (b) and (c). On contrast, the shear failure was not pronounced in the  
 227 steel tube confined RC specimens instead of evenly distributed cracks, as shown in Fig. 5 (f), (j) and  
 228 (h), indicating that the installation of longitudinal reinforcements improved the axial compressive

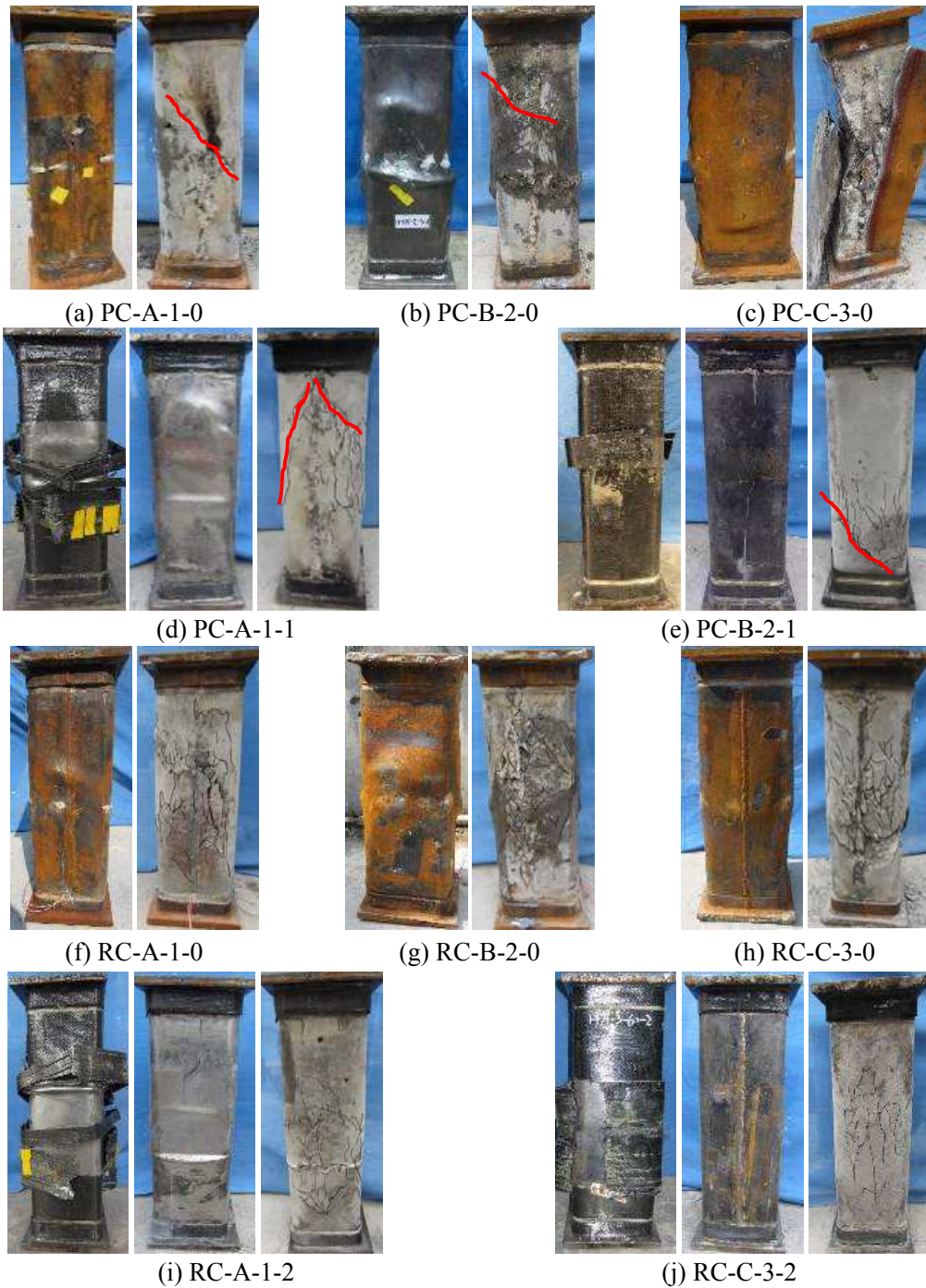


**Fig. 5.** Failure models of several representative confined concrete stub columns.

230

231

232

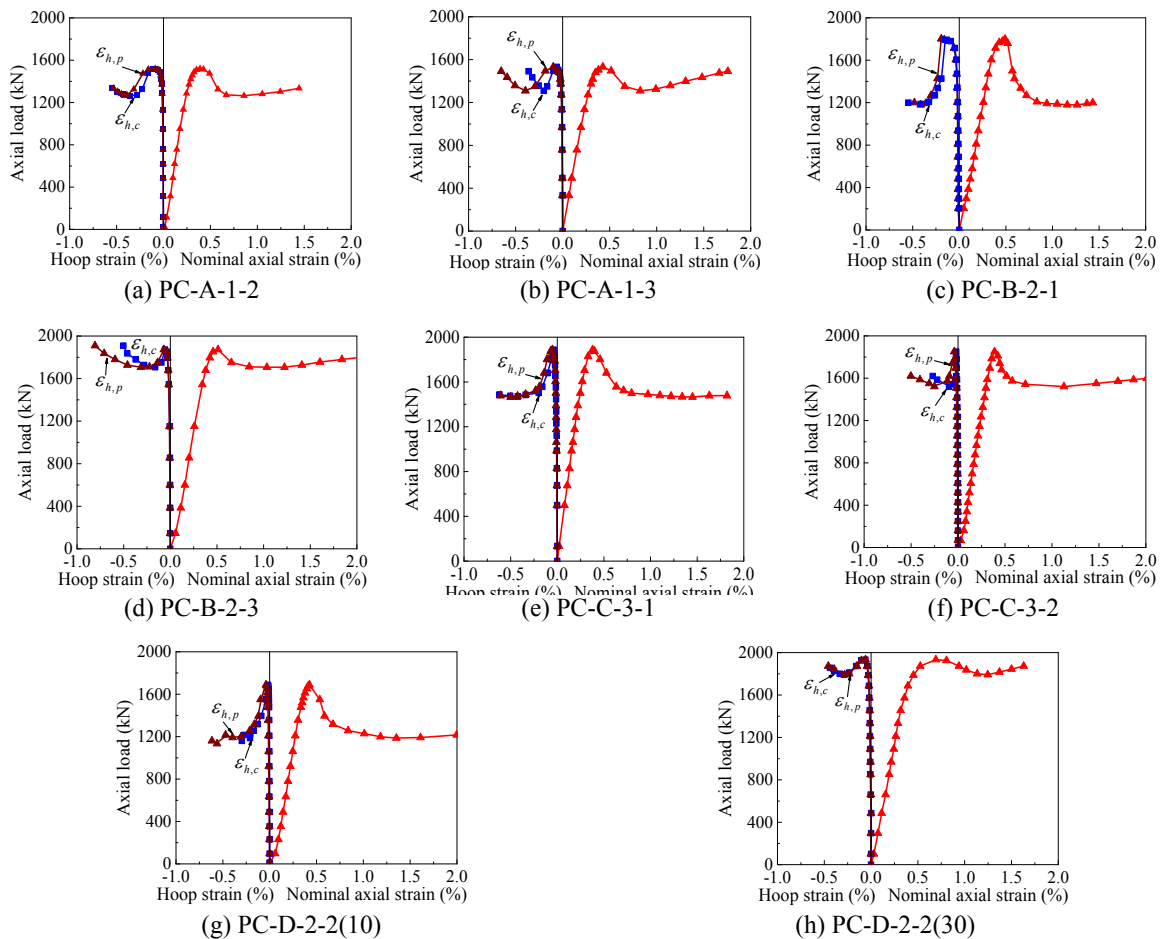
233

For the CFRP-steel confined concrete specimens, their ultimate failure was dominated by the hoop rupture of CFRP wrap (see Fig. 5 (d), (e), (i) and (j)). After the fracture of CFRP wrap, the local

234 buckling of steel tube near specimens' mid-height section was observed and then the whole specimen  
 235 failed. After removing the steel tubes, diagonal shear cracks still were observed in the surface of the  
 236 concrete core in the specimens, shown in Fig. 5 (d) and (e). However, the shear failure was avoided in  
 237 the CFRP-steel tube confined RC specimens (Fig. 5i and j), which confirms that the addition of  
 238 longitudinal reinforcement can play a beneficial effect on the axial compressive behaviour of CFRP-  
 239 steel tube confined concrete columns.

### 240 3.2 Axial load-strain behaviour

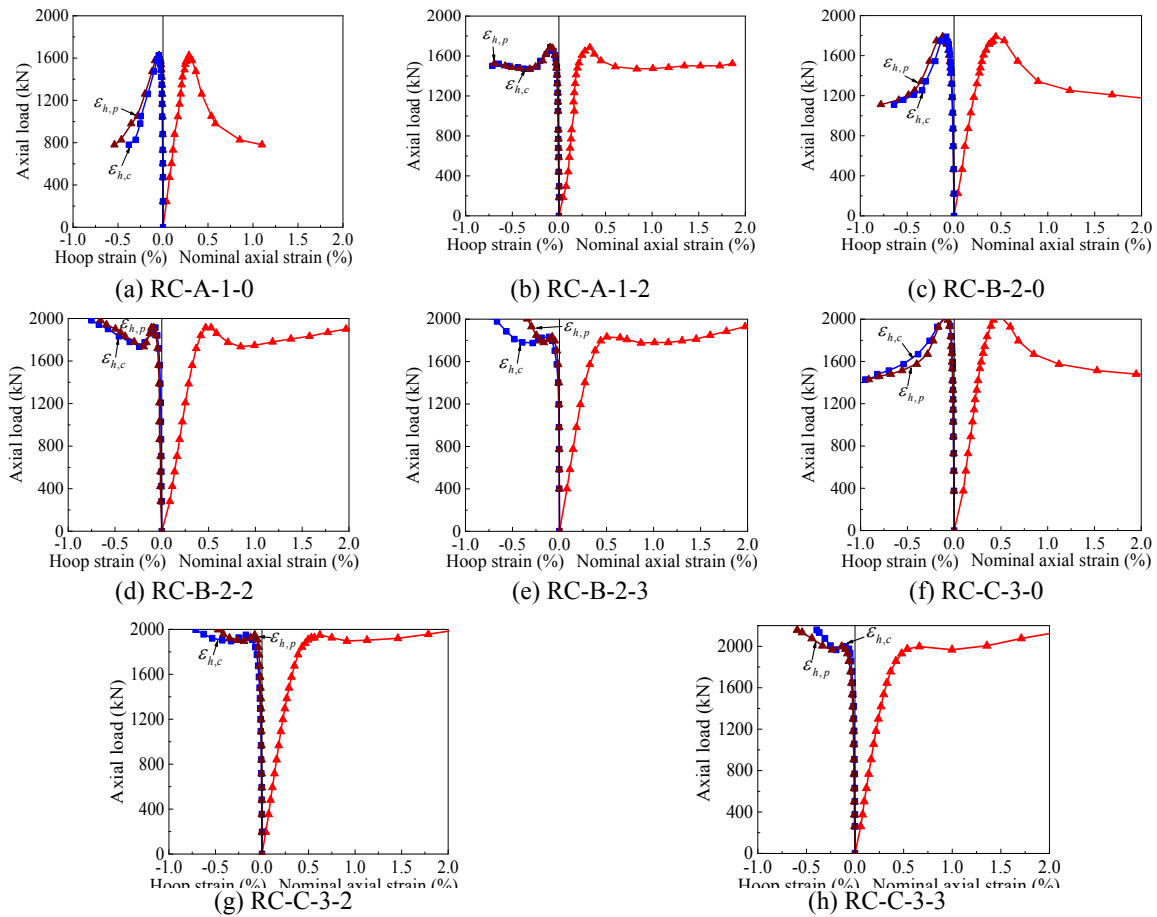
241 Figs. 6 and 7 depict the axial load-strain curves for several representative CFRP-steel tube  
 242 confined plain concrete specimens. In this study, the nominal axial strain was calculated as a ratio of  
 243 the axial shortening to the initial height of specimens, while the hoop strain was the average measured  
 244 strain by four hoop strain gauges installed on the corners or middle sections.



245 **Fig. 6.** Axial load-strain curves of confined plain concrete specimens.

246

247 Results show that all confined plain concrete and confined RC specimens deformed elastically at  
 248 the early stage. The axial deformation increased approximately linearly, and its increasing rate was  
 249 much greater than that of the lateral deformation. With the increasing of axial deformation, the lateral  
 250 deformation at the corners ( $\epsilon_{h,c}$ ) was smaller than the deformation at the middle of steel tube side at  
 251 the middle section ( $\epsilon_{h,p}$ ). This indicates that the concrete deformation at the corners of the steel tubes  
 252 was restrained well while the other deformations at the middle section are not well confined. The  
 253 bearing capacity of steel tube confined concrete specimens rapidly decreased after the specimens  
 254 reached their peak loads, and the axial load tended to stabilize when the peak load was reduced to a  
 255 certain load ranging from 50% to 90% of corresponding peak load.



256 **Fig. 7.** Axial load-strain curves of confined reinforced concrete specimens.  
 257

258 For both CFRP-steel confined plain concrete and confined RC specimens, their load carrying  
 259 capacity started to decrease after the specimens reached their first peak load. The lower the number of  
 260 layers of CFRP was, the larger the decrease of the bearing capacity was. When the curves decreased to

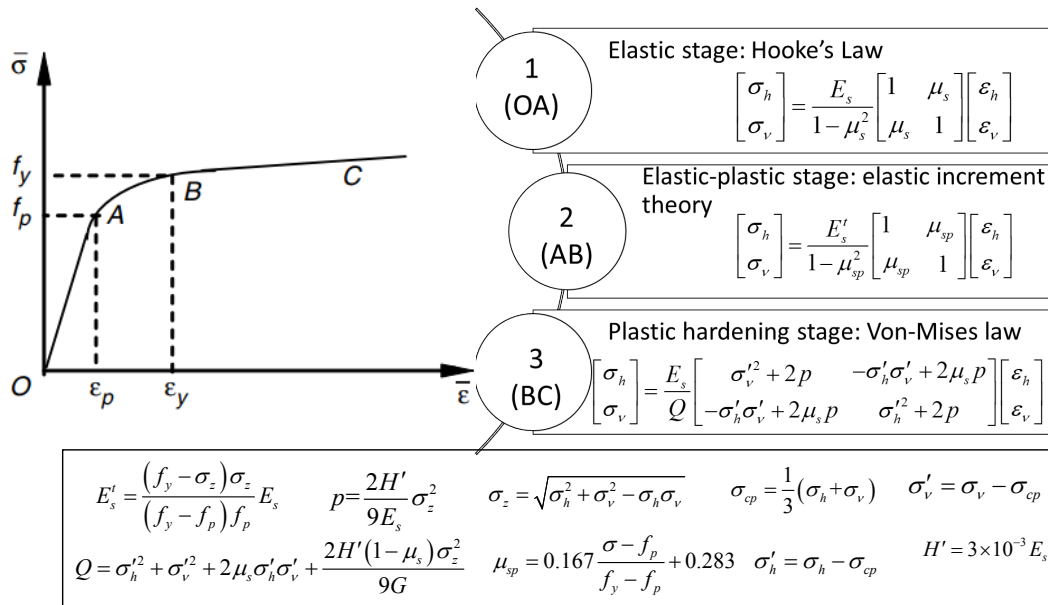
261 a certain extent, the hoop strain of the confined concrete started to increase and the curves began to  
 262 slightly rise. The greater the number of layers of CFRP wrap used in the specimens, the higher the  
 263 increase rate of the bearing capacity was. The softening phenomenon indicates that the confinement  
 264 effectiveness of FRP-steel tube in square section concrete specimens was relatively weak. The  
 265 softening phenomenon also occurred in CFRP-steel tube confined RC columns. However, the peak  
 266 load of the curves in the second rising section was generally larger than that of the confined plain  
 267 concrete specimens, e.g., PC-B-2-3 and RC-B-2-3 specimens. It shows that the deformability of  
 268 confined concrete specimens was improved after reinforcing rebars were added to the columns. This  
 269 improvement was more conducive to the development of the confinement effectiveness of the FRP-  
 270 steel composite tube so that the load carrying capacity of the columns increased.

### 271 3.3 Stress-strain relationship of steel tube

272 The confinement of steel tube to concrete core can be understood by analysing the longitudinal and  
 273 transverse stress of the steel tube. Referring to the literature [34], the stress of steel tube during loading  
 274 was determined based on the hoop and axial strain in the middle of the specimen. This brings a better  
 275 understanding of the confinement effectiveness of the steel tubes in the composite elements. Due to a  
 276 thin-walled steel tube was used in this study, the force perpendicular to the wall of steel tubes is small  
 277 and can be neglected. For this, the steel tube can be considered under the state of plane-stress [35]. Fig.  
 278 8 demonstrates the main calculation method of stress analysis of the steel tube at three stages. At the  
 279 elastic stage, the stress-strain relationship was assumed to obey the Hooke's law. An elastic increment  
 280 theory [34] was used to determine the stress of steel tube at the elastic-plastic stage (AB). The Von-  
 281 Mises yield criterion and the Prandtl-Reuss flow rule were adopted to analyse the behaviour of steel  
 282 tube at the plastic hardening stage (BC) [36]. In Fig. 8,  $\sigma_h$  and  $\varepsilon_h$  are the hoop stress and strain of steel  
 283 tube,  $\sigma_v$  and  $\varepsilon_v$  are the axial stress and strain of steel tube,  $\sigma_z$  is the equivalent stress of steel tube,  $\mu_s$  is  
 284 Poisson's ratio of steel in the elastic stage,  $E_s^t$  and  $\mu_{sp}$  are the tangent modulus and Poisson's ratio of  
 285 the steel in the elastoplastic stage,  $\sigma'_h$ ,  $\sigma'_v$  and  $\sigma_{cp}$  are the hoop and axial deviatoric stress of steel and  
 286 its mean stress,  $G$  is shear modulus of the steel,  $f_y$  and  $f_p$  are the steel yield strength and proportional  
 287 limit ( $0.8f_y$ ),  $\varepsilon_p$  and  $\varepsilon_y$  are the equivalent strain of steel corresponding to  $f_p$  and  $f_y$ , respectively.  $p$ ,  $H'$   
 288 and  $Q$  are defined parameters for the calculation [34].

289 It should be noted that the transverse and axial strains used for the stress analysis of steel tubes are  
 290 the strains at the middle of the mid-section of the steel tube. Fig. 9 shows the relationship between the  
 291 axial load and the stress of steel tube developed in several specimens. The tensile stress was  
 292 considered to have a negative sign in the stress analysis of steel tube. It was found that the axial stress

293 increased more quickly than the hoop stress at the early stage, and the growth rate gradually increased  
 294 with the increase of axial load. The yielding of steel tubes of the specimens was confirmed around  
 295 their first peak loads. After that point, the hoop stress of the steel tubes increased slowly, but in some  
 296 cases, a negative evolution was observed such as PC-B-2-1 and PC-D-2-2 (10). In these specimens,  
 297 the axial load decreased sharply too. This leads to the fact that the confinement of steel tube to  
 298 concrete core was effectively confined anymore after the significant expansion of concrete, which then  
 299 affected the bearing capacity of the specimens. In the CFRP-steel tube confined concrete specimens,  
 300 the hoop stress of the steel tube increased after the first peak load, and the load carrying capacity of the  
 301 specimens decreased slowly or increased slightly such as Specimen RC-C-3-3. This implies that the  
 302 FRP wrap can not only confine the concrete core, but can also confine the steel tube, which increases  
 303 the confinement effect of the steel tube on concrete core.



304  
305 **Fig. 8.** Stress analysis of steel tube [34].  
306

307 Besides, a similar test observation to that of the confined concrete specimens was confirmed in the  
 308 confined RC specimens. The confinement effectiveness of the FRP-steel tube on the concrete core was  
 309 stronger than those in the concrete specimens. For example, although the steel tube yielded in several  
 310 specimens, their bearing capacity kept increasing (see RC-C-3-3). This implies that the CFRP-steel  
 311 tube confined RC columns present better ductility and deformability compared to the confined plain  
 312 concrete columns.



313

314

315

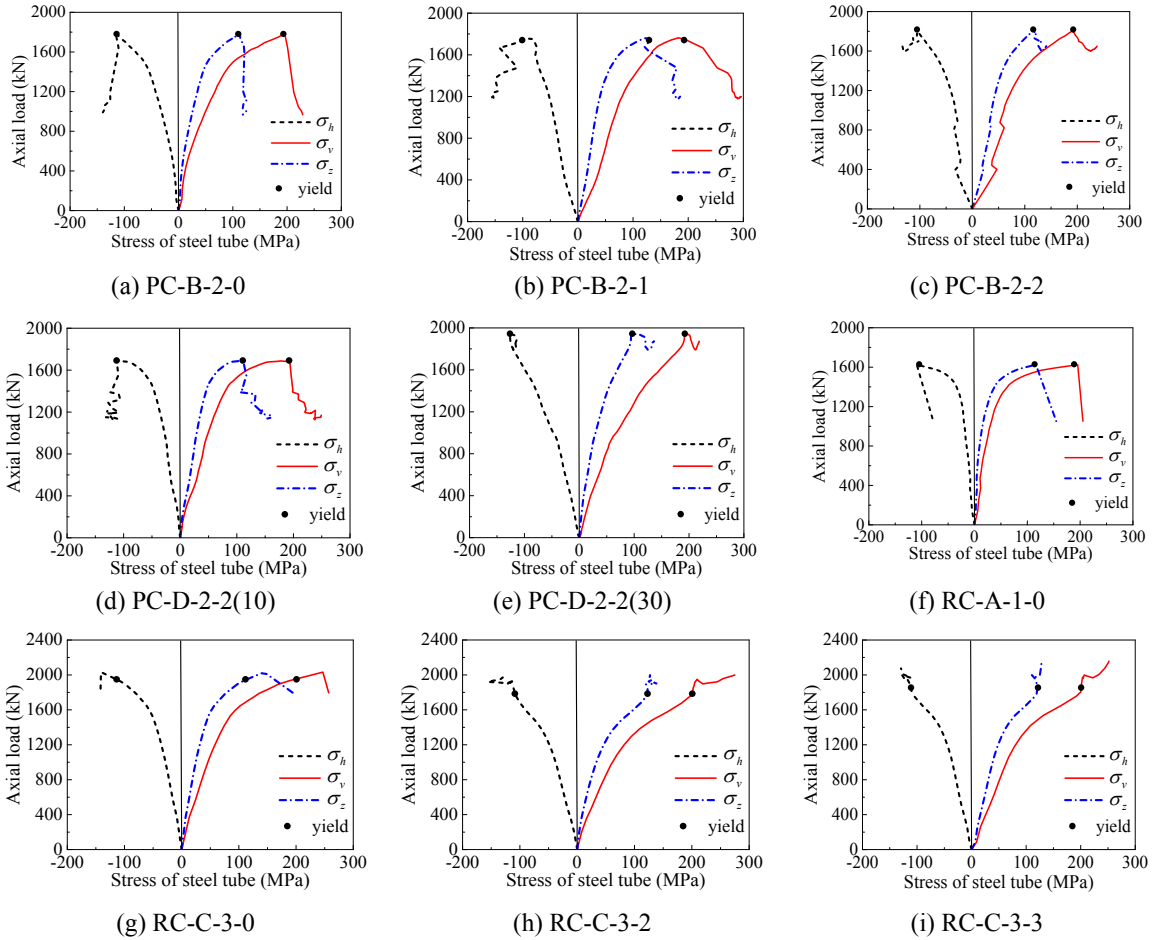


**Fig. 9.** Axial load-stress relationship of steel tube of representative specimens.

316

### 317 3.4 Stress-strain responses of confined concrete

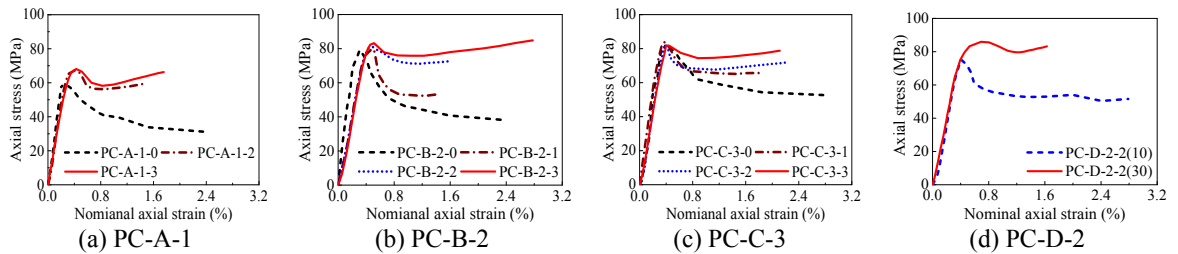
318 Applying the stress analysis of steel tube, the axial load resisted by steel tube can be discussed. In  
319 addition, the main fibres of CFRP wrap are only oriented in the hoop direction, so that the stiffness of  
320 the CFRP wrap in the direction perpendicular to the hoop direction is very small and can be ignored.  
321 When the axial stiffness of CFRP wrap is ignored, the load supported by concrete core can be  
322 calculated as the total load of the specimens deducted the load resisted by steel tube. Assuming the  
323 compressive stress on the entire section of concrete core is uniformly distributed, the compressive load  
324 of confined concrete can be calculated by dividing the deducted load by its cross-sectional area.  
325 Moreover, for confined RC specimens, the axial bearing contribution of the longitudinal reinforcement

326 should be deducted from the load resisted by whole column. In summary, the axial stress of confined  
 327 concrete can be obtained by,

$$328 \quad \sigma_c = \begin{cases} \frac{N - \sigma_v A_s}{A_c} & \text{for confined plain concrete} \\ \frac{N - \sigma_v A_s - f_a A_a}{A_c} & \text{for confined reinforced concrete} \end{cases} \quad (1)$$

329 where  $\sigma_c$  is the axial stress of confined concrete;  $N$  is the axial load resisted by whole column;  $\sigma_v$  is  
 330 the axial stress of steel tube;  $f_a$  is the yield strength of longitudinal reinforcement in the columns;  $A_s$ ,  
 331  $A_a$  and  $A_c$  are the cross-sectional areas of the steel tube, the longitudinal reinforcement and the  
 332 concrete core, respectively. Besides, the axial deformation of the confined concrete is believed to be  
 333 identical to the nominal axial strain of the specimens. Table.3 lists a summary on the calculated results  
 334 of the axial stress and measured strain of the concrete cores in the specimens, while Fig. 10 shows the  
 335 stress-strain curves of the confined concrete.

336 Results plotted in Fig. 10 demonstrate that the initial elastic moduli of the confined plain concrete  
 337 and RC are basically identical when compared within the same group. The first peak stress of the  
 338 CFRP-steel tube confined plain concrete specimens in Groups PC-A and PC-B (or Groups RC-A and  
 339 RC-B for confined RC specimens) were larger than those of the STCC specimens. The difference  
 340 among the CFRP-steel tube confined concrete or RC specimens was small, especially in Groups PC-C  
 341 and RC-C. This is explained by the fact that the  $B/t$  ratio of steel tube in Group A is large ( $B/t = 152$ )  
 342 indicating that the confining stress of the steel tubes was much smaller than others for it is prone to be  
 343 buckling failure. This also is the reason why the relatively weak confinement to suppress the  
 344 expansion deformation of the concrete cores in the specimens. When FRP wrap was used, the wrap  
 345 can not only restrain the lateral dilation of concrete core but also suppress the local buckling  
 346 deformation of steel tube, so that steel tube can continue to exert its confinement effect.



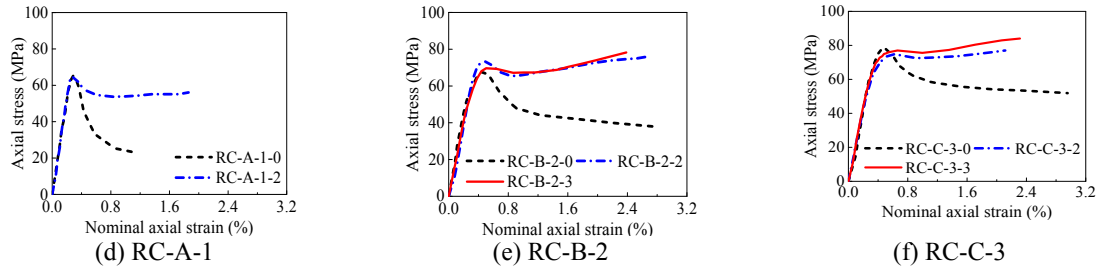


Fig. 10. Axial stress-strain curves of confined concrete.

Table 3. Summary of axial stress and axial strain of confined concrete.

Groups	Specimens	$f_{cc1}$ /MPa	$\varepsilon_{cc1}$ /%	$f_{cc2}$ /MPa	$\varepsilon_{cc2}$ /%
PC-A	PC-A-1-0	58.84	0.207	—	—
	PC-A-1-2	67.50	0.389	59.32	1.45
	PC-A-1-3	68.11	0.428	66.30	1.76
PC-B	PC-B-2-0	79.23	0.313	—	—
	PC-B-2-1	79.89	0.490	53.33	1.43
	PC-B-2-2	80.90	0.498	72.79	1.62
	PC-B-2-3	83.24	0.512	84.86	2.78
PC-C	PC-C-3-0	82.14	0.418	—	—
	PC-C-3-1	83.86	0.378	65.67	1.82
	PC-C-3-2	82.28	0.388	72.02	2.24
	PC-C-3-3	81.71	0.402	78.80	2.12
PC-D	PC-D-2-2 (10)	75.03	0.425	51.56	2.78
	PC-D-2-2 (30)	85.94	0.692	83.24	1.63
RC-A	RC-A-1-0	63.95	0.274	—	—
	RC-A-1-2	64.87	0.300	50.86	1.86
RC-B	RC-B-2-0	67.80	0.445	—	—
	RC-B-2-2	73.24	0.526	76.28	2.72
	RC-B-2-3	69.67	0.503	78.24	2.39
RC-C	RC-C-3-0	78.47	0.489	—	—
	RC-C-3-2	74.84	0.622	76.98	2.12
	RC-C-3-3	76.98	0.662	84.02	2.31

Note:  $f_{cc1}$  and  $\varepsilon_{cc1}$  are the first peak stress and corresponding nominal axial strain of confined concrete;  $f_{cc2}$  and  $\varepsilon_{cc2}$  are the ultimate stress and corresponding nominal axial strain of confined concrete at the rupture of FRP wrap.

In the confined plain concrete and RC specimens, following the first peak axial stress, the effective confining stresses of the steel tube and FRP wrap in the square section are relatively small. Similar to previous research, the confinement is effective only in a limited confinement area in square concrete. It cannot prevent the expansion deformation of concrete in the non-effective confinement area. This was the reason why the stress-strain curves of the concrete exhibited different degrees of softening. The softening segment was smaller as the number of CFRP layers increased, and the stress-strain curves of confined concrete after this stage increased with varying degrees. This indicates that the

360 lateral expansion deformation of the concrete core increased and the confining stress of CFRP wrap  
361 increased, leading to an increase in confining stress to the concrete core. The axial stress of the  
362 confined concrete increased until the hoop rupture of CFRP wrap. The slope of the secondary  
363 ascending branch of the axial stress-strain curves increased with the number of layers of CFRP.  
364 Besides, the corner radius of the steel tube has a significant influence on the stress-strain curves of  
365 confined concrete, as shown in Fig. 10 (d). Results show that the strength and ductility of confined  
366 concrete corresponding to a steel tube with a corner radius of 30 mm is significantly better than that of  
367 the specimen with a corner radius of 10 mm.

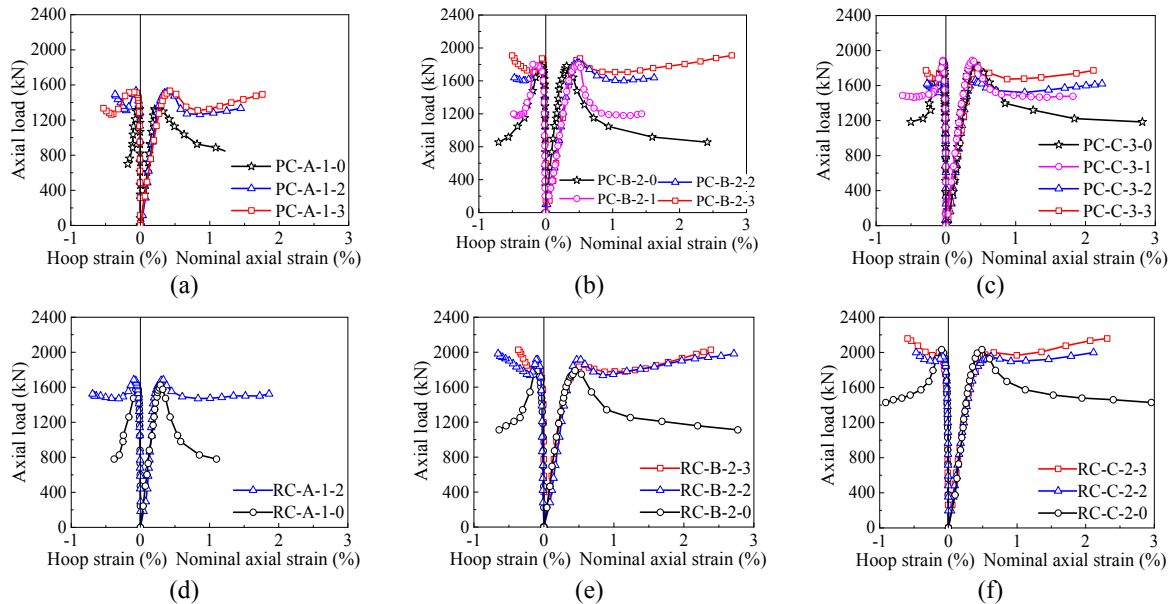
368 In addition, it is worth mentioning that the size effect also is an important affecting factor of the  
369 composite confined columns especially for square columns. The hoop strain of CFRP wrap is non-  
370 uniformly distributed along the circumferential direction. The hoop strain of CFRP wrap at the corners  
371 varies with the sectional size of square columns, leading to a considerable influence on the  
372 compressive behaviour of confined concrete. To the best of the authors' knowledge, the size effect in  
373 square FRP-steel tube confined plain concrete or RC columns has not been understood well. However,  
374 the study conducted by Wang et al. [37] on square FRP-confined RC columns can provide a  
375 significant reference to this issue. The experimental results [37] revealed that the compressive strength  
376 of square FRP-confined concrete decreased with cross-section size, while ultimate axial strain was  
377 influenced little by section size. Therefore, the size effect also may have an important impact on the  
378 axial compressive behaviour of square FRP-STCC elements, which deserves further concerns in the  
379 future.

### 380 **3.5. Effects of test parameters**

#### 381 (1) Effect of the number of CFRP layers

382 Fig. 11 depicts the effect of the number of CFRP layers on the axial load-strain behaviour of steel  
383 tube confined concrete specimens and CFRP-steel tube confined concrete specimens, where the lateral  
384 strain is the measured strain at the corners of the specimens. Results show that the number of CFRP  
385 layers affects the first peak loads and corresponding axial strain. When the number of CFRP layers  
386 increased, the degree of post-peak softening of the specimens decreased significantly. After the first  
387 peak load, the curves of the CFRP-steel tube confined concrete specimens were much smoother than  
388 those of the steel tube confined concrete specimens. The more CFRP layers were used, the more  
389 gradual the curves exhibited and the higher the ultimate axial deformation of the specimens was. A  
390 significant increase was confirmed in the axial load-strain responses of the specimens with 3-ply FRP  
391 wrap after their softening stage, which is demonstrated by the fact that the bearing capacities of the

392 specimens even exceeded their first peak loads in some cases. This indicates that the CFRP wrap can  
 393 work with steel tube together to provide an effective confinement to concrete core, where the steel  
 394 tube can effectively prevent the local and sharp damage of FRP wrap while the FRP can confine the  
 395 steel tube at large hoop deformations.



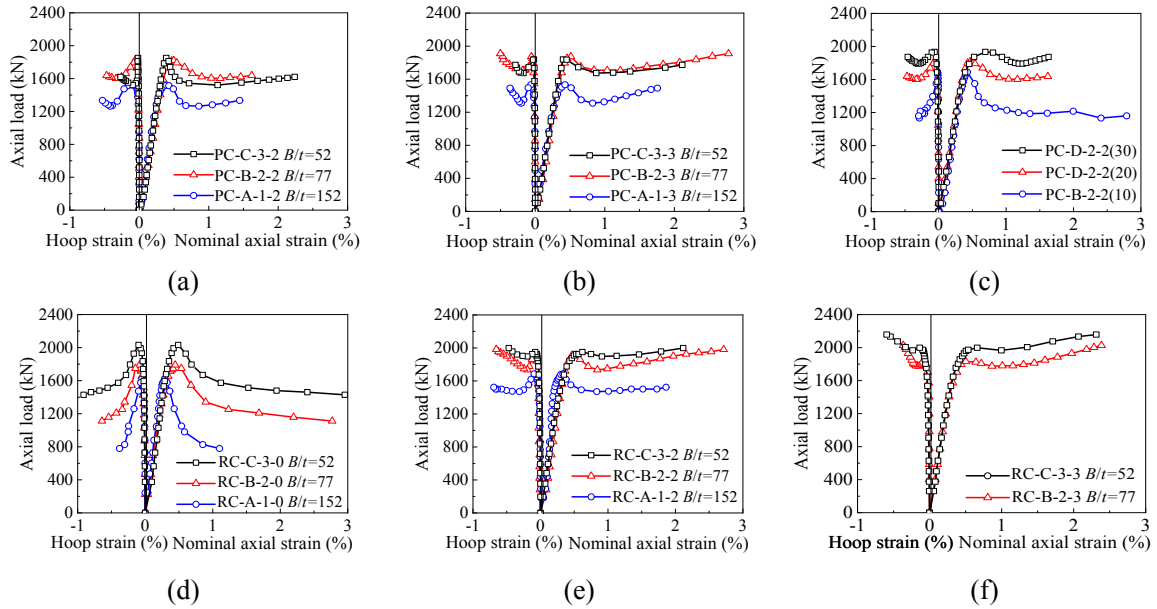
396 **Fig. 11.** Effect of the number of CFRP layers.

397  
 398 For the CFRP-steel tube confined RC specimens, the elastic behaviour and first peak load of the  
 399 specimens are not significantly affected by the number of CFRP layers. The first peak loads were  
 400 slightly larger than those of steel tube confined specimens. After first peak load, the axial load-strain  
 401 curves of the CFRP-steel tube confined RC specimens continued to rise until the rupture of CFRP  
 402 wrap. The ultimate bearing capacities of the CFRP-steel tube confined RC specimens with 3-ply FRP  
 403 wrap corresponding to the rupture of FRP wrap were larger than their first peak loads. This means that  
 404 with the increase of the number of CFRP layers, the co-confinement effectiveness of CFRP-steel tube  
 405 to the square concrete core is significantly enhanced.

406 (2) Effect of the width-to-thickness ( $B/t$ ) ratio of steel tubes

407 As shown in Fig. 12, the specimens with higher  $B/t$  ratio present smaller bearing capacities.  
 408 Compared to the load capacity of the specimens using a  $B/t$  ratio of 152.0, the first peak loads of both  
 409 the specimens with  $B/t$  ratios of 52.0 and 77.0 were higher. This means that the  $B/t$  ratio of the steel  
 410 tube has a significant influence on the bearing capacity of the CFRP-steel tube confined concrete  
 411 specimens. This is similar to the cases of the steel tube confined concrete elements. Besides, the

412 smaller the  $B/t$  ratio was, the higher the load carrying capacity and ductility of the stub columns were.  
 413 A similar result was found in the CFRP-steel tube confined RC specimens, but it seems that the  $B/t$   
 414 ratio has a slightly stronger influence on the first peak loads and on the ductility of the specimens.



415 **Fig. 12.** Effect of width-to-thickness on axial load-strain curves at different FRP layers.

416

417 (3) Effect of corner radius at sectional corners

418 The effects of three levels of the corner radius of steel tube were experimentally study, i.e., 10 mm,  
 419 20 mm and 30 mm, respectively, as shown in Fig. 11 (c). The results show that the ultimate load of the  
 420 specimens increases significantly with the increase of the corner radius. The softening behaviour of  
 421 the curves after the first peak load was significantly reduced and slowed down as the radius increases.  
 422 This presents the potential to improve the mechanical properties of square sectional confined plain  
 423 concrete or RC columns by properly increasing the corner radius of column section. This is explained  
 424 by the fact that more concrete core can be effectively confined in the columns, which is illustrated  
 425 later in the study.

426

427 **4. Discussion on confinement mechanism**

428 **4.1 Effective confinement of steel tube and FRP in confined square section**

429 With reference to the cases in traditional square stirrup confined concrete, the effective

430 confinement mechanism of either steel tube confined concrete or FRP-steel tube confined concrete is  
 431 presented in Fig. 13. In these sections, only the concrete in the area enclosed by four parabola lines  
 432 with initial tangent lines 45° from the corresponding sides of the section (see Fig. 13 (a)) can be  
 433 effectively confined. This is a significant difference compared to the cases in circular confined- plain  
 434 concrete or RC. Pham and Hadi [38] proposed a confinement mechanism of the concrete in confined  
 435 square columns, which is shown in Figs. 13 (b) and (c). The confining stress at the corners is much  
 436 larger than that at the four sides since the curvature radius of sectional sides is much greater than that  
 437 of the corners. The confining stress  $f_r$  at the corners is given as

$$438 \quad f_r = \frac{\sigma_{h,j}}{R} \quad (2)$$

439 where  $\sigma_{h,j}$  is the hoop stress of a confining jacket at the corners;  $R$  is the corner radius.

440 According to Section 3.3, the confining stress provided by the steel tube  $f_{r,s}$  is expressed as

$$441 \quad f_{r,s} = \frac{\sigma_h}{R} \quad (3)$$

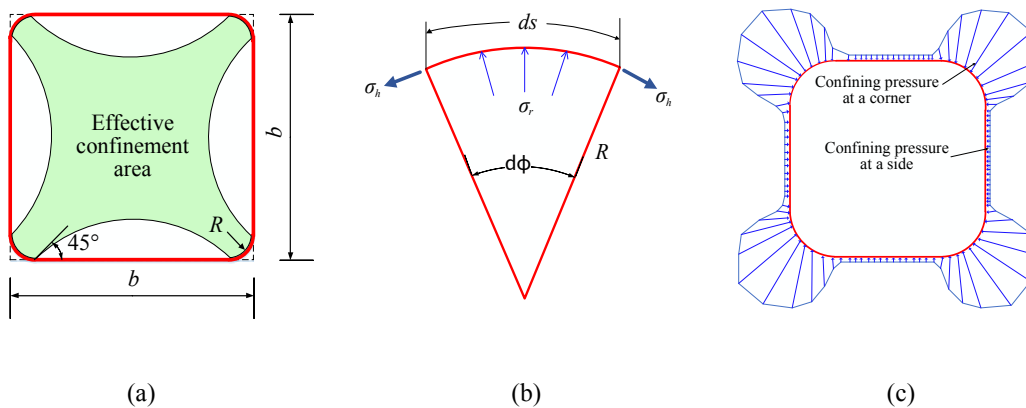
442 where  $\sigma_h$  is the hoop stress of steel tube at the corners.

443 Therefore, according to Fig. 13 (c), the confining stress of FRP wrap  $f_{r,frp}$  is given as

$$444 \quad f_{r,frp} = \frac{\sigma_{h,frp}}{R+t} = \frac{E_{frp}\varepsilon_{f,c}t_{frp}}{R+t} \quad (4)$$

445 where  $\sigma_{h,frp}$  and  $\varepsilon_{f,c}$  are the hoop stress and hoop strain of the FRP wrap at corners, respectively;

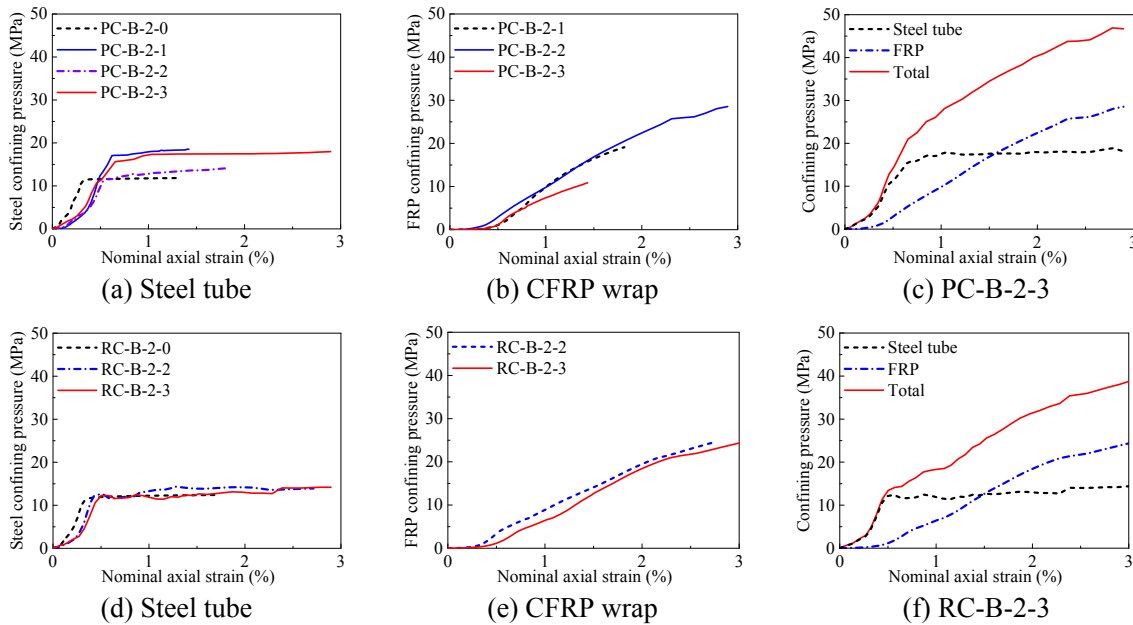
446  $E_{frp}$  and  $t_{frp}$  are the Young's modulus and thickness of FRP wrap, respectively.



447 **Fig. 13.** The confinement of square confined concretes: (a) effective confining area of confined concrete;  
 448 (b) stress distribution; and (c) confinement mechanism of FRP confined concrete [38].

449

450 Fig. 14 shows the evolution of the confining pressure of the steel tube and the CFRP wrap in the  
451 specimens, as well as the total confining pressure with the increasing nominal axial strain of the stub  
452 columns. Results show that the confining pressure of the steel tube increases rapidly at the initial stage  
453 of loading, and then increases slowly or almost remains constant during the later period. This indicates  
454 that the confining pressure of steel tube to the concrete core is limited after the yielding of the steel  
455 tube. On the other hand, the confining pressure provided by CFRP wrap was not high at the initial  
456 loading. Due to the increase of the lateral deformation of the steel tube, the FRP wrap started to  
457 provide a higher confining stress, for example, from an axial strain of 0.004 to 0.006. After that, the  
458 confining pressure of the CFRP wrap increased until the rupture of the FRP wrap. No obvious  
459 difference was found between the CFRP-steel tube confined plain concrete and RC specimens.



460 **Fig. 14.** Confining pressure provided by the steel tube and the CFRP wrap.

461

#### 462 4.2 Confinement mechanism of square FRP-steel tube confined concrete/reinforced concrete

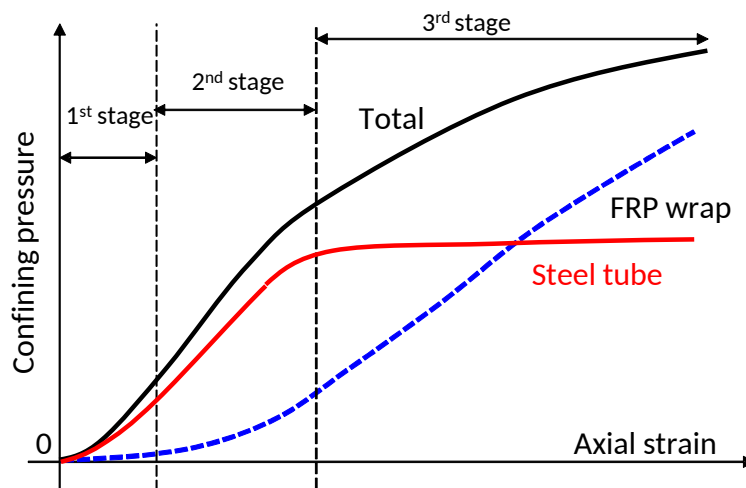
463 Based on the above analysis, Fig. 15 shows an ideal evolution of various confining pressures in  
464 FRP-steel tube confined plain concrete and RC columns, which explains the confinement mechanism  
465 of the composite tube to concrete core. The evolution of the confining pressure provided by steel tube  
466 and FRP wrap in the composite columns is similar to that observed in FRP-confined CFT specimens  
467 reported by Hu *et al.* [1]. However, the confinement mechanism of the specimens still is different from  
468 that in FRP-confined CFT specimens for the steel tube does not directly carry the axial load.



469 According to Fig. 15, the confinement actions in FRP-steel tube confined plain concrete and RC  
470 columns can be divided into three stages as follows,

471 (1) 1<sup>st</sup> stage – steel tube confinement stage

472 In this stage, the confining pressure of the concrete core comes mostly from the confinement of  
473 steel tube, while the confinement from FRP wrap can be nearly neglected. This is because the test  
474 specimens are only subjected to a small axial compression load, resulting in a very small lateral  
475 expansion in the concrete core at this stage. There are few obvious differences between the confined  
476 plain concrete and the confined RC columns as the stirrups were limited and only to erect the  
477 longitudinal reinforcements in the study. Therefore, it is believed that the stirrups only provide a quite  
478 small confinement to the concrete core. The small lateral deformation induced by a small axial strain  
479 in the concrete core does not need the confinement action of FRP wrap. Therefore, if the potential  
480 deformation of the confined plain concrete or RC columns remains at this level, the additional FRP  
481 confinement is not necessary from the point of view of the mechanical performance of the elements.



482

483 **Fig. 15.** Ideal confinement in FRP-steel tube confined concrete columns.

484

485 (2) 2<sup>nd</sup> stage – FRP-steel tube co-confinement stage

486 The second stage can be considered as a co-confinement stage consisting of both the confining  
487 pressures from steel tube and FRP wrap. However, as shown in Fig. 15, the two types of confining  
488 pressures increase at different rates depending primarily on their hoop stiffness. This stage is similar to  
489 the case in FRP-confined CFT columns [1]. The total confining pressure increases rapidly in this stage,  
490 as the lateral deformation of concrete core starts to rapidly increase. Based on the experimental  
491 investigation in the present study, the second stage can be delimited to a nominal axial strain of around

492 0.006. The FRP and steel tube work together in this stage and delay their respective fracture or local  
493 buckling due to the contribution of each partner.

494 (3) 3<sup>rd</sup> stage – FRP-dominated confinement increasing stage

495 The third stage of the confinement of FRP-steel tube confined concrete is dominated by FRP  
496 confinement. In this stage, the increasing total confining pressure to inner concrete comes mainly from  
497 the increasing confinement of FRP wrap, as the confinement of the steel tube keep almost a constant  
498 level after its yielding. The high strength feature of FRP materials becomes apparent at this stage. At  
499 the same time, the behaviour of the FRP material itself still is highly elastic, and the confining  
500 pressure of the FRP wrap can keep a similar increasing rate to that of the second stage. Therefore, at  
501 this stage, the increasing rate of the total confining pressure of onfined concrete or RC columns at this  
502 stage becomes smaller than that of the second stage, which is similar to the previous research results of  
503 FRP-confined CFT columns [1].

## 504 **5. Proposal for predicating axial bearing capacity of composite square stub columns**

505 Referring to previous research [39, 40], the superposition principle was used to predict the axial  
506 bearing capacity of CFRP-steel tube confined plain concrete or RC stub columns ( $N_u$ ), which is given  
507 as

$$508 \quad N_u = f_{CFS}A_c + f_a A_a \quad (5)$$

509 where  $A_c$  and  $A_a$  are the cross-sectional areas of concrete core and longitudinal reinforcement,  
510 respectively;  $f_a$  is the yield strength of longitudinal reinforcement; and  $f_{CFS}$  is the compressive  
511 strength of CFRP-steel tube confined concrete.

512 Based on the test results reported in this paper, a superposition calculation method is applied to  
513 predict the axial bearing capacity of CFRP-steel tube confined plain concrete or RC stub columns,  
514 consisting of the contribution of steel tube and FRP wrap. The discussion on the steel tube, FRP and  
515 FRP-steel tube confined concrete is presented in the following sections.

### 516 **(1) For steel tube confined concrete**

517 According to the literature, the calculation model for steel stirrup-confined concrete strength  $f_{cc}$   
518 proposed by Mander et al. [41] is given as

$$519 \quad f_{cc} = f_{co} \left( 1 + 2.254 \sqrt{1 + \frac{7.94f_r}{f_{co}}} - 2\frac{f_r}{f_{co}} - 2.254 \right) \quad (6)$$

520 where  $f_{co}$  is the compressive strength of unconfined concrete, and  $f_r$  is the confining pressure provided  
521 by steel stirrups.

522 Referring to this model, the ultimate compressive strength of steel tube confined concrete ( $f_{CS}$ ) is  
 523 given as

$$524 \quad f_{CS} = f_{co} \left( 1 + 2.254 \sqrt{1 + \frac{7.94 f_{r,s}}{f_{co}}} - 2 \frac{f_{r,s}}{f_{co}} - 2.254 \right) \quad (7)$$

525 where  $f_{r,s}$  is the confining pressure provided by steel tube calculated based on a static equilibrium,  
 526 which is given as

$$527 \quad f_{r,s} = \frac{2\sigma_h t}{B - 2t} \quad (8)$$

$$528 \quad \sigma_h = \beta f_y \quad (9)$$

529 where  $\sigma_h$  is the hoop stress of the steel tube corresponding to the peak load of confined concrete  
 530 columns;  $B$  and  $t$  are the width and thickness of square steel tube, respectively;  $\beta$  is a reduction factor  
 531 related to the yielding strength of steel  $f_y$ . Previous studies [39, 40] proposed a similar prediction  
 532 model and suggested the factor  $\beta$ , which is influenced by the width-thickness ratio of steel tube  
 533 ranging from 50 to 100. However, based on the test results in this study, an average value of 0.62 was  
 534 taken for the simplification of the calculations.

## 535 (2) For FRP-confined concrete

536 Based on the model proposed by Lam and Teng [42], the ultimate strength of square FRP-confined  
 537 concrete ( $f_{CF}$ ) is suggested as

$$538 \quad f_{CF} = f_{co} \left[ 1 + k_1 k_{s1} \left( \frac{f_{r,FRP}}{f_{co}} \right) \right] \quad (10)$$

539 In this equation,  $f_{r,FRP}$  is the confining pressure provided by FRP wrap to an equivalent circular  
 540 column [42], and the confinement effectiveness coefficient  $k_1 = 3.3$ , same as defined in Lam and Teng  
 541 model [43] for uniformly confined concrete. Referring to Ref. [42],  $k_{s1}$  is defined as a shape factor  
 542 calculated as

$$543 \quad k_{s1} = 1 - \frac{2 (B_0 - 2R)^2}{3B_0^2 - (4 - \pi)R^2} \quad (11)$$

544 where  $R$  is the corner radius of inner concrete. Referring to the literature [38, 44], the confinement  
 545 effectiveness is reduced at the corner of concrete [45]. Therefore, the confining pressure of FRP to  
 546 concrete ( $f_{r,FRP}$ ) is expressed as

547 
$$f_{r,FRP} = \frac{n t_{frp} k_c k_r E_{frp} \varepsilon_{h,rup}}{D} \quad (12)$$

548 where  $n$  is the number of layers of FRP wrap;  $D$  is an equivalent diameter which is taken as  $\sqrt{2}B_0$  in  
 549 this paper;  $t_{frp}$  is the thickness of FRP wrap;  $E_{frp}$  and  $\varepsilon_{h,rup}$  are the elastic modulus and the hoop  
 550 rupture strain of FRP wrap. Referring to the method introduced by Hadi et al. [44], a corner-effect  
 551 coefficient  $k_c$  was introduced to reduce the stronger confining stress at the corner. The factor was  
 552 defined as the ratio of the sum of the corner length to the sectional perimeter and given as

553 
$$k_c = \frac{\pi R}{2B_0 - (4 - \pi)R} \quad (13)$$

554 Besides, to consider the effect of the large curvature of the corners on FRP wrap leading to a stress  
 555 concentration of the FRP wrap, the reduction factor  $k_r$  is introduced. Based on the literature [45], the  
 556 factor is taken as

557 
$$k_r = \left(1 - 0.2121 \times \frac{\sqrt{2}}{2}\right) \frac{2R}{B_0} + 0.2121 \times \frac{\sqrt{2}}{2} \quad (14)$$

558 The FRP efficiency factor ( $k_\varepsilon$ ) is defined as the ratio of recorded hoop rupture strain of FRP ( $\varepsilon_{h,rup}$ )  
 559 to the ultimate tensile strain of FRP obtained from flat coupon tests ( $\varepsilon_{frp}$ ), which is shown in Eq. (15)  
 560 and taken as 0.33 based on the test results of the study.

561 
$$k_\varepsilon = \varepsilon_{h,rup} / \varepsilon_{frp} \quad (15)$$

### 562 **(3) For FRP-steel tube confined concrete**

563 The steel tube confinement is generally regarded as an active confinement because the confining  
 564 pressure provided by steel tube almost remains constant after the yielding of steel tube. On contrast,  
 565 the FRP confinement is generally considered as a passive confinement because the confining pressure  
 566 provided by FRP wrap increases continuously with the lateral dilation of concrete. Therefore, the FRP-  
 567 steel composite confinement might be a confinement type between active confinement and passive  
 568 confinement. Theoretically, the steel tube-FRP composite confinement in the study can be regarded as  
 569 one integral confinement since the two confining materials are well bonded based on the tests in the  
 570 study. However, up to now the theoretical model of FRP-steel composite confined concrete is not  
 571 researched well. In the present study, a simplified superposition calculation method was used based on  
 572 the understanding of steel-confined concrete and FRP-confined concrete. As a start, the simplified  
 573 method is relatively rough but easier to be understood by structural engineers.

574 Based on the superposition principle, the ultimate strength of square FRP-steel tube confined

575 concretes can be calculated as a total strength consisting of the contribution components of FRP wrap  
 576 and steel tube, which is given as

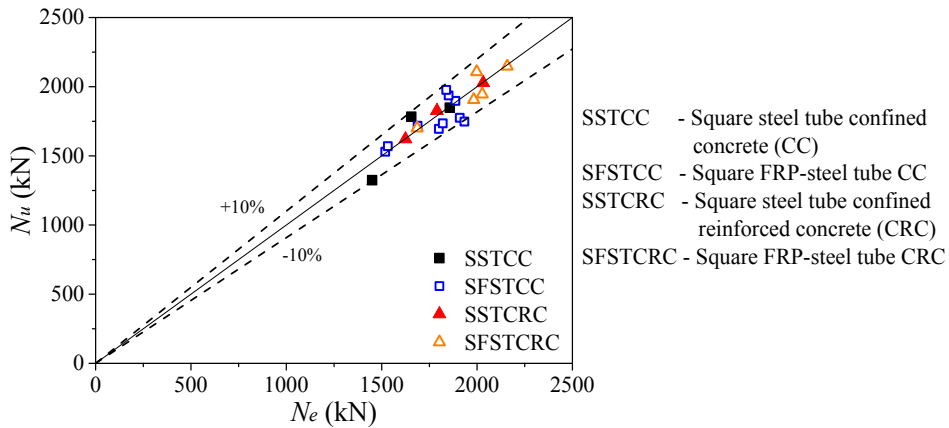
$$577 \quad f_{CFS} = f_{co} \left[ 1 + \left( 2.254 \sqrt{1 + \frac{7.94f_{r,s}}{f_{co}}} - 2\frac{f_{r,s}}{f_{co}} - 2.254 \right) + k_1 k_{s1} \left( \frac{f_{r,FRP}}{f_{co}} \right) \right] \quad (16)$$

578 Taking Eqs. (7) and (16) into Eq. (5), the axial bearing capacities of steel tube confined concrete  
 579 stub columns and FRP-steel tube confined concrete stub columns are expressed as

$$580 \quad N_u = \begin{cases} f_{co} \left( 1 + 2.254 \sqrt{1 + \frac{7.94f_{r,s}}{f_{co}}} - 2\frac{f_{r,s}}{f_{co}} - 2.254 \right) A_c + f_a A_a \\ f_{co} \left[ 1 + \left( 2.254 \sqrt{1 + \frac{7.94f_{r,s}}{f_{co}}} - 2\frac{f_{r,s}}{f_{co}} - 2.254 \right) + k_1 k_{s1} \left( \frac{f_{r,FRP}}{f_{co}} \right) \right] A_c + f_a A_a \end{cases} \quad (17)$$

581 Fig. 16 compares the prediction results of proposed model with the experimental results in this  
 582 study. Regardless of the confinement types, the proposed model evaluates the ultimate bearing  
 583 capacities of these confined plain concrete and RC columns with a great agreement.

584



585

586 **Fig. 16.** Comparisons between calculated and experimental results.

587

588 In addition to the axial bearing capacity, ultimate axial strain of composite stub columns is a very  
 589 important parameter. For square STCC specimens, as shown in Table 3, the strain capacity increases  
 590 with the thickness of steel tube because a thicker steel tube usually can provide a larger confinement to  
 591 concrete core. Moreover, the installation of longitudinal reinforcements also can improve strain  
 592 capacity. For square FRP-STCC specimens, the strain capacity generally increases with the thickness  
 593 of steel tube, the number of layers of FRP wrap and the installation of longitudinal reinforcements.  
 594 Therefore, the confinements from steel tube and FRP wrap as well as the advantageous effects of  
 595 longitudinal reinforcement should be considered when predicting the strain capacities of square STCC  
 596 stub columns and square FRP-STCC columns, which is expected to be studied in the future.

597

## 598 **6. Concluding remarks**

599 This paper presented an experimental study to understand the monotonic axial compressive behaviour  
600 and confinement mechanism of square CFRP-steel tube confined concretes. The confinement from  
601 steel tube and CFRP wrap enhances the ultimate strength and ductility of core concrete. CFRP  
602 wrapping effectively constrains the deformation of steel tube, which delays its outward local buckling  
603 and constrains the continuous dilation of core concrete at the stage of large deformation. Based on this  
604 study, the following conclusions can be drawn:

605 1. The CFRP-steel tube confinement is highly effective in improving the bearing capacity and ductility  
606 of concrete columns, especially for plain concrete. The number of layers of CFRP wrap has a  
607 significant effect on the failure of the confined reinforced concrete columns. The width-to-thickness  
608 ratio of the steel tube is also a key factor affecting the axial bearing capacity of confined concrete  
609 columns.

610 2. The post-peak softening phenomenon of square confined concretes was observed in the specimens.  
611 However, the softening degree of the columns was improved by using a thicker CFRP wrap. The  
612 effect of the CFRP wrap is more pronounced for the CFRP-steel tube confined concrete columns with  
613 a larger width-to-thickness ratio of steel tube.

614 3. Through a detailed stress analysis, the stress-strain curves of the concrete core confined by  
615 composite action of steel tube and CFRP wrap were provided. The mechanical properties of the  
616 concrete core was greatly improved by the composite confinement. The study explained the  
617 confinement mechanism of the steel tube and the FRP wrap in confined plain or reinforced concrete  
618 columns, and the role of steel tube and CFRP wrap in each load stage, which provides a basis for the  
619 establishment of a calculation model of the bearing capacity for the columns. The three stages of the  
620 confinement mechanism include a steel tube confinement stage which is similar to steel tube confined  
621 concrete, and a CFRP-steel tube co-confinement stage in which the total confinement pressure  
622 increases rapidly due to the effective co-confinement from steel tube and CFRP wrap, and a FRP-  
623 dominated confinement increasing stage when FRP wrap keeps an effective confinement to steel tube  
624 and concrete core to resist axial compressive load.

625 4. Based on previous studies and discussion on the strength models for confined concrete, through a  
626 superposition principle considering the confinement of steel tube and CFRP wrap, this paper proposed  
627 a simplified calculation model to predict the axial bearing capacity of CFRP-steel tube confined plain  
628 concrete and reinforced concrete stub columns. Comparing with test results, the accuracy and

629 reliability of proposed model was confirmed.

630 Compared with CFRP, GFRP wrap may be more suitable to work together with the steel tube than  
631 CFRP in FRP-STCC elements, because of GFRP materials' low cost, greater fracture strain. The  
632 potential galvanic corrosion issues also will be eliminated. In the future, the axial compressive  
633 behaviour of GFRP-STCC elements will be investigated.

634

### 635 Acknowledgements

636 The authors of the paper appreciate the support from the National Key R&D Program of China (No.  
637 2017YFC0703000), the National Natural Science Foundation of China (Nos. 51778102 and  
638 51978126), the Fundamental Research Funds for the Central Universities (No. DUT18LK35), and the  
639 Natural Science Foundation of Liaoning Province of China (No. 20180550763).

640

641

### 642 Notation

643	$A_a$	cross-sectional area of longitudinal reinforcement
644	$A_c$	cross-sectional area of concrete core
645	$A_s$	cross-sectional areas of steel tube
646	$B$	width of steel tube
647	$B_0$	width of concrete core
648	$D$	equivalent diameter
649	$E_{frp}$	elastic modulus of FRP
650	$E_s$	elastic modulus of steel
651	$E_s^t$	tangent modulus steel in the elastoplastic stage
652	$H$	height of the specimen
653	$f_a$	yield strength of longitudinal reinforcement
654	$f_y$	yield strength of steel tube
655	$f_p$	proportional limit of steel tube
656	$f_{co}$	compressive strength of unconfined concrete
657	$f_r$	confining pressure
658	$f_{r,s}$	confining pressure provided by steel tube
659	$f_{r,FRP}$	confining pressure provided by FRP wrap
660	$f_{CF}$	compressive strength of FRP-confined concrete
661	$f_{CS}$	compressive strength of steel tube confined concrete
662	$f_{CFS}$	compressive strength of FRP-steel tube confined concrete
663	$f_{cc1}$	first peak stress of confined concrete
664	$f_{cc2}$	ultimate stress of confined concrete corresponding to the rupture of FRP wrap
665	$G$	shear modulus of the steel
666	$k_1$	confinement effectiveness coefficient
667	$k_{s1}$	shape factor
668	$k_c$	corner-effect coefficient

669	$k_r$	reduction factor considering stress concentration at corner
670	$k_\varepsilon$	FRP efficiency factor
671	$n$	the number of FRP layer
672	$N$	axial load resisted by the composite column
673	$N_u$	axial bearing capacity of the composite column
674	$R$	corner radius
675	$t$	thickness of steel tube
676	$t_{frp}$	thickness of FRP wrap
677	$\beta$	reduction factor
678	$\mu_s$	Poisson's ratio of steel in the elastic stage
679	$\mu_{sp}$	Poisson's ratio of steel in the elastoplastic stage
680	$\sigma_h$	hoop stress of steel tube
681	$\sigma_v$	axial stress of steel tube
682	$\sigma_c$	axial stress of confined concrete
683	$\sigma_{h,j}$	hoop stress of a confining jacket
684	$\sigma_z$	equivalent stress of steel tube
685	$\varepsilon_p$	equivalent strain of steel tube corresponding to $f_p$
686	$\varepsilon_y$	equivalent strain of steel tube corresponding to $f_y$
687	$\varepsilon_h$	hoop strain of steel tube
688	$\varepsilon_v$	axial strain of steel tube
689	$\varepsilon_{frp}$	ultimate tensile strain of FRP coupon
690	$\varepsilon_{h,rupt}$	hoop rupture strain of FRP wrap
691	$\varepsilon_{cc1}$	nominal axial strain of confined concrete corresponding to $f_{cc1}$
692	$\varepsilon_{cc2}$	nominal axial strain of confined concrete corresponding to $f_{cc2}$
693		

## 694 References

- 695 [1] Hu YM, Yu T, Teng JG. FRP-confined circular concrete-filled thin steel tubes under axial compression.  
696 J Compos Constr 2011;15(5):850–60.
- 697 [2] Xu TX, Liu JP, Wang XD, Guo Y, Chen YF. Behaviour of short CFRP-steel composite tubed  
698 reinforced normal and high strength concrete columns under eccentric compression. Eng Struct  
699 2020;205:110096.
- 700 [3] Sakaino K, Ishibashi H. Experimental studies on concrete filled square steel tubular short columns  
701 subjected to cyclic shearing force and constant axial force. J Struct Constr Eng 1985;353: 81–91.
- 702 [4] Xiao Y, Tomii M, Sakino K. Experimental study on design method to prevent shear failure of  
703 reinforced concrete short circular columns by confining in steel tube. Trans Japan Concr Inst  
704 1986;8:535–42.
- 705 [5] Yan B, Liu J, Zhou X. Axial load behavior and stability strength of circular tubed steel reinforced  
706 concrete (SRC) columns. Steel Compos Struct 2017;25(5):545–56.
- 707 [6] Aboutaha RS, Machado RI. Seismic resistance of steel-tubed high-strength reinforced-concrete  
708 columns. J Struct Eng 1999;125(5):485–94.
- 709 [7] Zhou XH, Liu JP, Wang XD, Chen YF. Behavior and design of slender circular tubed-reinforced-  
710 concrete columns subjected to eccentric compression. Eng Struct 2016;124:17–28.
- 711 [8] Mei H, Kioussis PD, Ehsani MR, Saadatmanesh H. Confinement effects on high-strength concrete.  
712 Struct J 2001;98(4):548–53.
- 713 [9] Zhou XH, Liu JP. Seismic behavior and shear strength of tubed RC short columns. J Constr Steel Res  
714 2010;66:385–97.
- 715 [10] Einde L V D, Zhao L, Seible F. Use of FRP composites in civil structural applications. Constr Build  
716 Mater 2003;17(6-7):389–403.



- 717 [11] Bai YL, Dai JG, Mohammadi M, Lin G, Mei SJ. Stiffness-based design-oriented compressive stress-  
718 strain model for large-rupture-strain (LRS) FRP-confined concrete. *Compos Struct*  
719 2019;223(2019):110953.
- 720 [12] Wang YL, Cai GC, Li YY, Waldmann D, Si Larbi A, Tsavdaridis KD. Behavior of circular fiber-  
721 reinforced polymer-steel-confined concrete columns subjected to reversed cyclic loads: experimental  
722 studies and finite-element analysis. *J Struct Eng* 2019;145(9):04019085.
- 723 [13] Cao Q, Tao J, Wu Z, Ma ZJ. Behavior of FRP-steel confined concrete tubular columns made of  
724 expansive self-consolidating concrete under axial compression. *J Compos Constr* 2017;21(5):04017037.
- 725 [14] Bai YL, Yan ZW, Ozbakkaloglu T, Han Q, Dai JG, Zhu DJ. Quasi-static and dynamic tensile  
726 properties of large-rupture-strain (LRS) polyethylene terephthalate fiber bundle. *Constr Build Mater*  
727 2020;232(2020):117241.
- 728 [15] Wang YL, Chen GP, Wan BL, Cai GC, Zhang YW. Behavior of circular ice-filled self-luminous FRP  
729 tubular stub columns under axial compression. *Constr Build Mater* 2020;232(2020):117287.
- 730 [16] Wang YL, Wang YS, Wan BL, Han BG, Cai GC, Li ZZ. Properties and mechanisms of self-sensing  
731 carbon nanofibers/epoxy composites for structural health monitoring. *Compos Struct*  
732 2018;200(2018):669–78.
- 733 [17] Wang YL, Wang YS, Wan BL, Han BG, Cai GC, Chang RJ. Strain and damage self-sensing of basalt  
734 fiber reinforced polymer laminates fabricated with carbon nanofibers/epoxy composites under tension.  
735 *Compos Part A Appl Sci Manuf* 2018;113(2018):40–52.
- 736 [18] Zeng JJ, Gao WY, Duan ZJ, Bai YL, Guo YC, Ouyang LJ. Axial compressive behavior of  
737 polyethylene terephthalate/carbon FRP-confined seawater sea-sand concrete in circular columns. *Constr*  
738 *Build Mater* 2020;234(2020):117383.
- 739 [19] Cao Q, Tao J, Ma ZJ, Wu Z. Axial Compressive Behavior of CFRP-Confined Expansive Concrete  
740 Columns. *ACI Struct J* 2017;114(2):475–85.
- 741 [20] Park JW, Choi SM. Structural behavior of CFRP strengthened concrete-filled steel tubes columns  
742 under axial compression loads. *Steel Compos Struct* 2013;14(5):453–72.
- 743 [21] Xiao Y, He W, Choi KK. Confined concrete-filled tubular columns. *J Struct Eng* 2005;131(3):488–97.
- 744 [22] Tao Z, Wang Z, Han L, Uy B. Fire performance of concrete-filled steel tubular columns strengthened  
745 by CFRP. *Steel Compos Struct* 2011;11(4):307–24.
- 746 [23] Wang Z, Yu Q, Tao Z. Behaviour of CFRP externally-reinforced circular CFST members under  
747 combined tension and bending. *J Constr Steel Res* 2015;106:122–37.
- 748 [24] Yu T, Hu YM, Teng JG. Cyclic lateral response of FRP-confined circular concrete-filled steel tubular  
749 columns. *J Constr Steel Res* 2016;124:12–22.
- 750 [25] Park JW, Hong YK, Choi SM. Behaviors of concrete filled square steel tubes confined by carbon fiber  
751 sheets (CFS) under compression and cyclic loads. *Steel Compos Struct* 2010;10(2):187–205.
- 752 [26] Liu L, Lu Y. Axial bearing capacity of short FRP confined concrete-filled steel tubular columns. *J*  
753 *Wuhan Univ Technol* 2010;25(3):454–8.
- 754 [27] Teng JG, Hu YM, Yu T. Stress-strain model for concrete in FRP-confined steel tubular columns. *Eng*  
755 *Struct* 2013;49(2):156–67.
- 756 [28] Wang QL, Zhao Z, Shao YB, Li QL. Static behavior of axially compressed square concrete filled  
757 CFRP-steel tubular (S-CF-CFRP-ST) columns with moderate slenderness. *Thin Wall Struct*  
758 2017;110:106–22.
- 759 [29] Lin SY. Seismic performance of FRP-steel composite tube confined RC columns. MS Thesis of  
760 Harbin Institute of Technology, Harbin, China, 2003. (In Chinese)
- 761 [30] Zhao J, Cai GC, Cui L, Si Larbi A, Tsavdaridis DK. Deterioration of basic properties of the materials  
762 in FRP-strengthening RC structures under ultraviolet exposure. *Polymers* 2017; 9(9), 402.
- 763 [31] Huang PD. Cyclic axial compression mechanical behavior study of GFRP-steel composite tube  
764 confined RC stub columns. MS Thesis of Dalian University of Technology, Dalian, China, 2006. (In  
765 Chinese)
- 766 [32] GB 50608-2010. Technical code for infrastructure application of FRP composites. Ministry of housing  
767 and urban-rural development of the People's Republic of China, 2010. (In Chinese).
- 768 [33] GB/T 228-2002. Metallic materials-tensile testing at ambient temperature. General Administration of  
769 Quality Supervision, Inspection and Quarantine of the People's Republic of China, 2002. (In Chinese)

- 770 [34] Zhang S, Guo L, Ye Z, Wang Y. Behavior of steel tube and confined high strength concrete for  
771 concrete-filled RHS tubes. *Adv Struct Eng* 2005;8(2):101–16.
- 772 [35] Zhang S, Guo L, Tian H. Eccentrically loaded high strength concrete-filled square steel tubes. In:  
773 Proceedings of the international conference on advances in structures. Sydney, Australia, 2003.
- 774 [36] Chen WF, Saleeb AF. Constitutive equations for engineering materials: Vol.1—Elasticity and  
775 modeling. UK: John Wiley & Sons, Inc., 1982.
- 776 [37] Wang Z, Wang D, Smith ST, Lu D. CFRP-confined square RC columns. I: Experimental  
777 investigation. *J Compos Constr* 2012;16:150–60.
- 778 [38] Pham TM, Hadi MN. Stress prediction model for FRP confined rectangular concrete columns with  
779 rounded corners. *J Compos Constr* 2013;18(1):04013019.
- 780 [39] Qi H, Guo L, Liu J, Gan D, Zhang S. Axial load behavior and strength of tubed steel reinforced-  
781 concrete (SRC) stub columns. *Thin Wall Struct* 2011;49(9):1141–50.
- 782 [40] Liu J, Zhou X. Behavior and strength of tubed RC stub columns under axial compression. *J Constr*  
783 *Steel Res* 2010;66(1):28–36.
- 784 [41] Mander JB, Priestley MJ, Park R. Theoretical stress-strain model for confined concrete. *J Struct Eng*  
785 1988;114(8):1804–26.
- 786 [42] Lam L, Teng JG. Design-oriented stress-strain model for FRP-confined concrete in rectangular  
787 columns. *J Reinf Plast Comp* 2003;22(13):1149–86.
- 788 [43] Lam L, Teng JG. Design-oriented stress-strain model for FRP-confined concrete. *Constr Build Mater*  
789 2003;17(6-7):471–89.
- 790 [44] Hadi MN, Pham TM, Lei X. New method of strengthening reinforced concrete square columns by  
791 circularizing and wrapping with fiber-reinforced polymer or steel straps. *J Compos Constr*  
792 2012;17(2):229–38.
- 793 [45] Campione G, Miraglia N. Strength and strain capacities of concrete compression members reinforced  
794 with FRP. *Cement Concrete Comp* 2003;25(1):31–41.
- 795  
796  
797

**Declaration of Competing Interest**

We declare that we do not have any commercial or associative interest that represents a conflict of interest in connection with the work submitted.

**CRedit authorship contribution statement**

**Yanlei Wang:** Conceptualization, Funding acquisition, Supervision, Writing - original draft, Writing - review & editing. **Gaochuang Cai:** Conceptualization, Supervision, Writing - original draft, Writing - review & editing. **Amir Si Larbi:** Methodology, Writing - review & editing. **Danièle Waldmann:** Methodology, Validation, Writing - review & editing. **Konstantinos Daniel Tsavdaridis:** Methodology, Validation, Writing - review & editing. **Jianghua Ran:** Data curation, Investigation, Methodology, Validation.